超 导 体

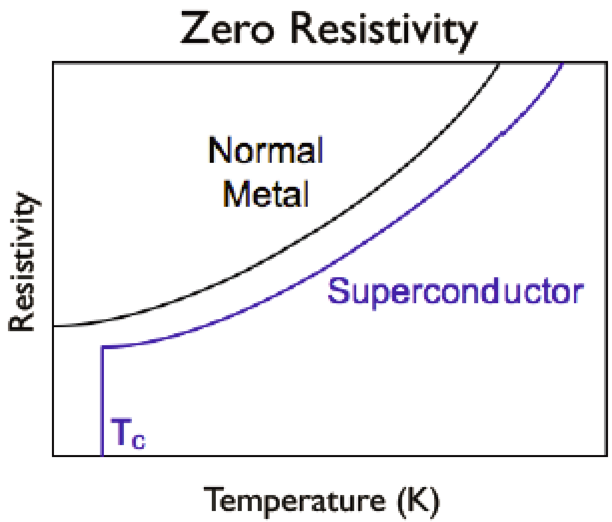
Zero Resistivity
Normal
Metal
Superconductor
Tc
Resistivity
Temperature (K)

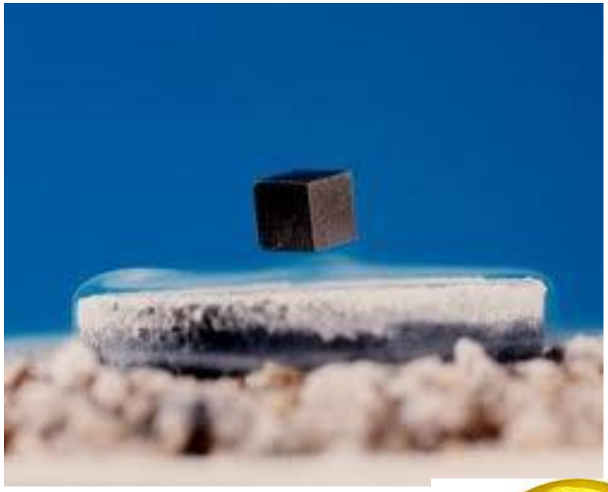

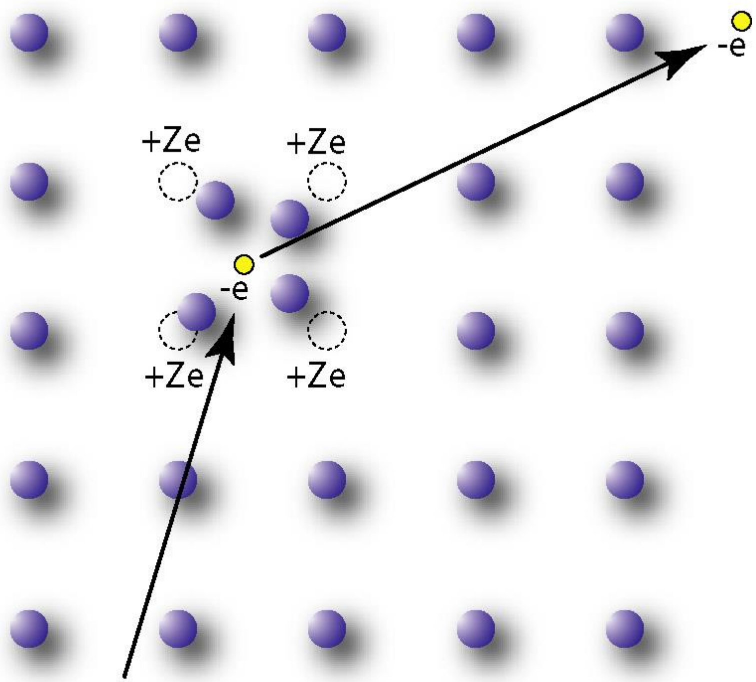
-e
+Ze
+Ze
-e
+Ze
+Ze

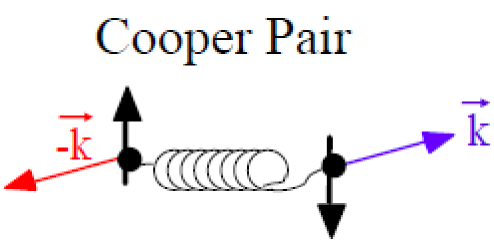
Cooper Pair
-k
k

Onnes

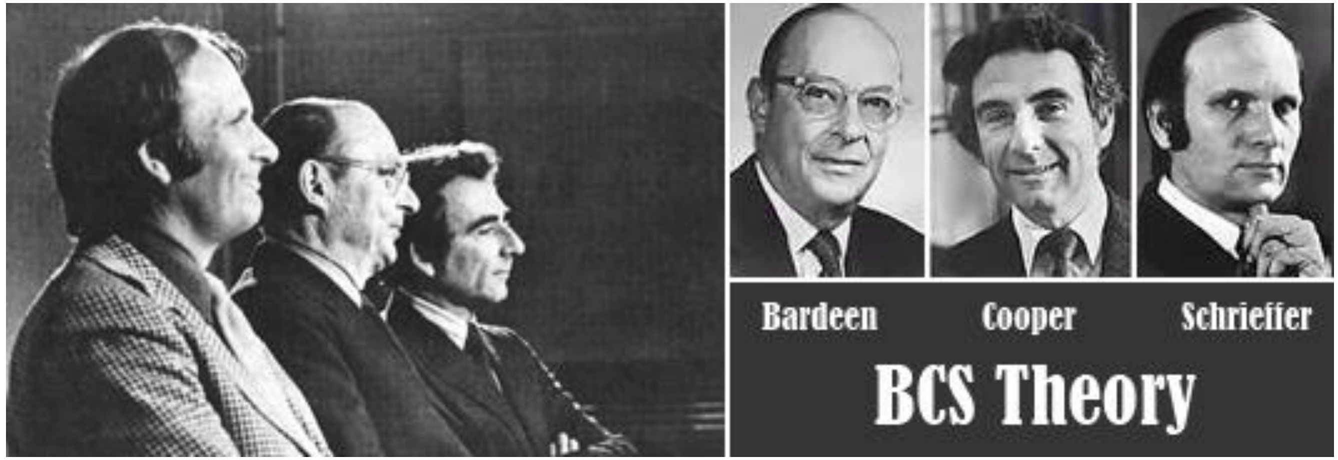

缪勒和贝德诺尔茨

超 导 体

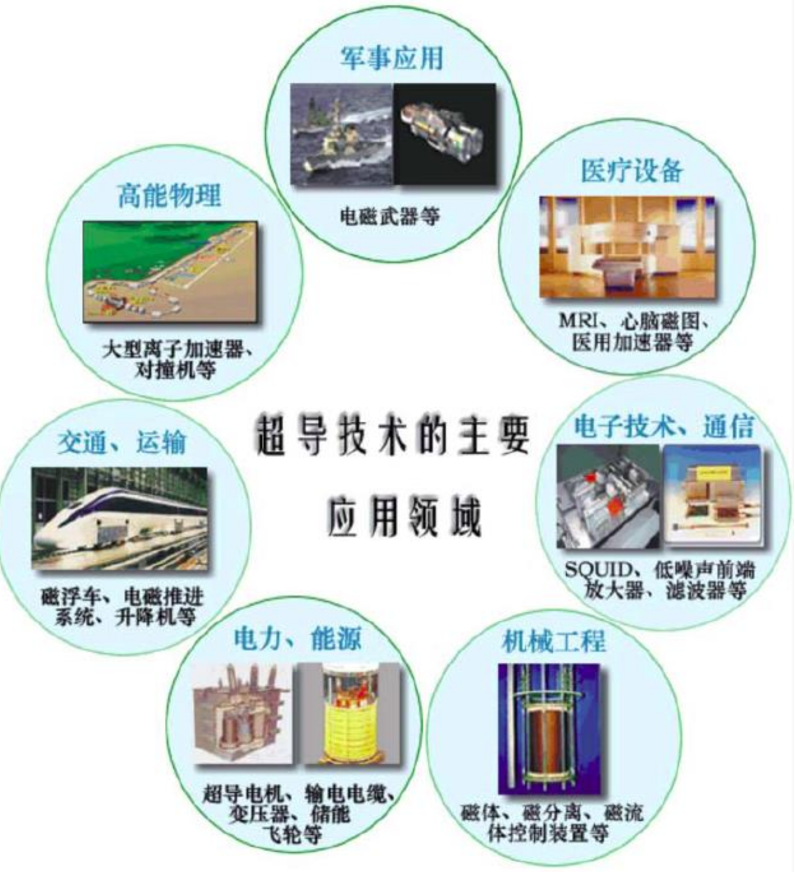

超导技术的主要应用领域
军事应用
电磁武器等
高能物理
大型离子加速器、对撞机等
医疗设备
MRI、心脑磁图、医用加速器等
交通、运输
磁浮车、电磁推进系统、升降机等
电子技术、通信
SQUID、低噪声前端放大器、滤波器等
电力、能源
超导电机、输电电缆、变压器、储能飞轮等
机械工程
磁体、磁分离、磁流体控制装置等

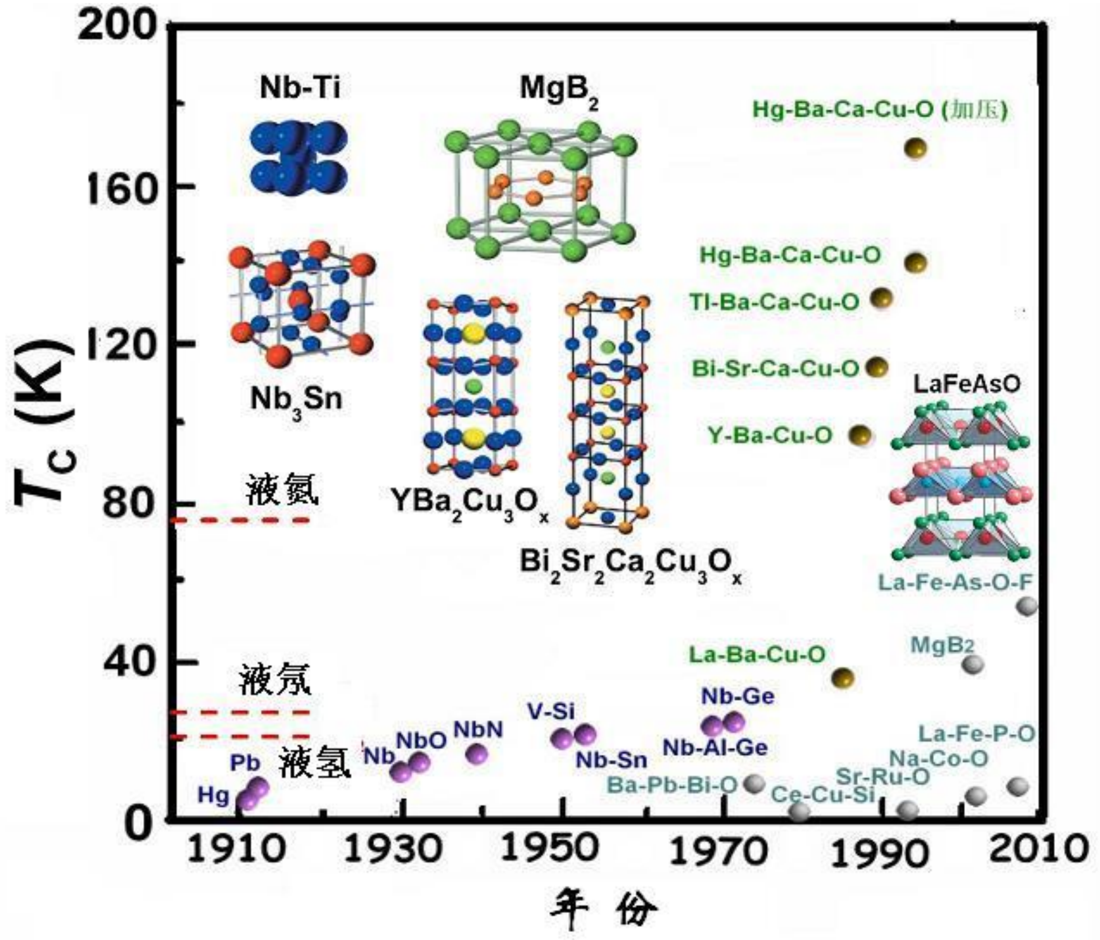

Nb-Ti
MgB2
Nb3Sn
YBa2Cu3Ox
Bi2Sr2Ca2Cu3Ox
Hg-Ba-Ca-Cu-O (加压)
Hg-Ba-Ca-Cu-O
Tl-Ba-Ca-Cu-O
Bi-Sr-Ca-Cu-O
Y-Ba-Cu-O
LaFeAsO
La-Fe-As-O-F
MgB2
La-Ba-Cu-O
Nb-Ge
Nb-Al-Ge
V-Si
Nb-Sn
NbN
NbO
Nb
Pb
Hg
Ba-Pb-Bi-O
Ce-Cu-Si
Sr-Ru-O
Na-Co-O
La-Fe-P-O
液氮
液氖
液氢
Tc (K)
0
40
80
120
160
200
1910
1930
1950
1970
1990
2010
年 份

Reason for SC - formation of Cooper Pairs (two electrons form a Boson)

Pairs condense into macroscopic quantum SC state

Cooper Pair

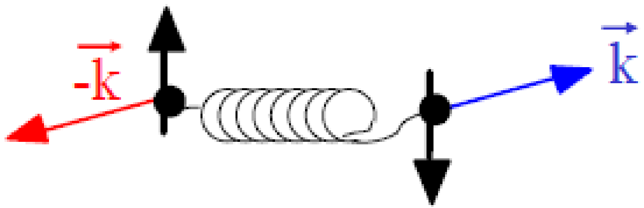

Conventional SC - pairing mediated by electron-phonon interaction

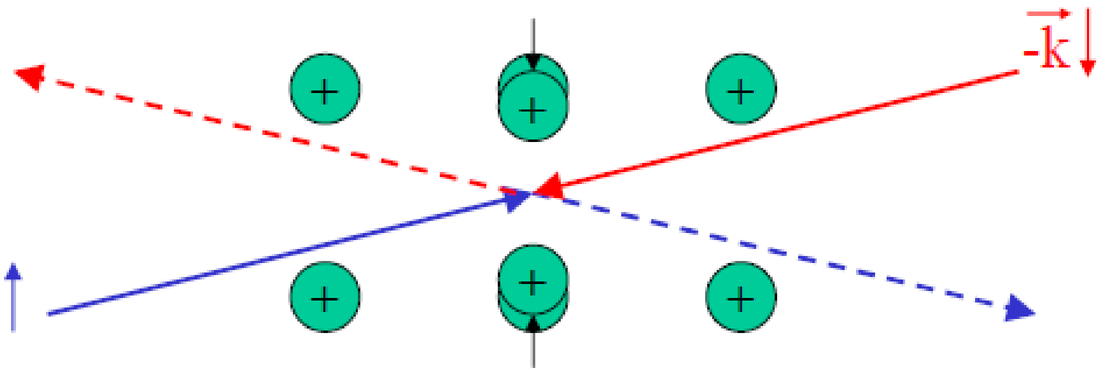

The superconducting gap ?

Energy to remove an electron from system - 1/2 of binding energy of the pair

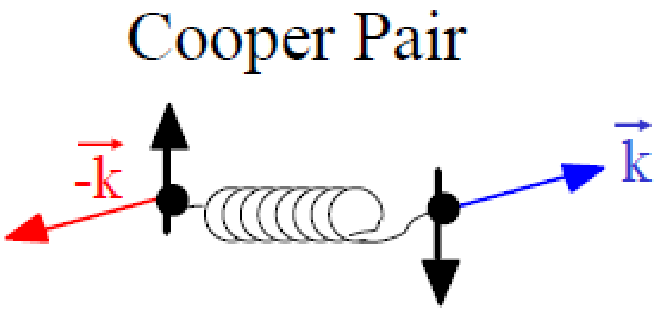

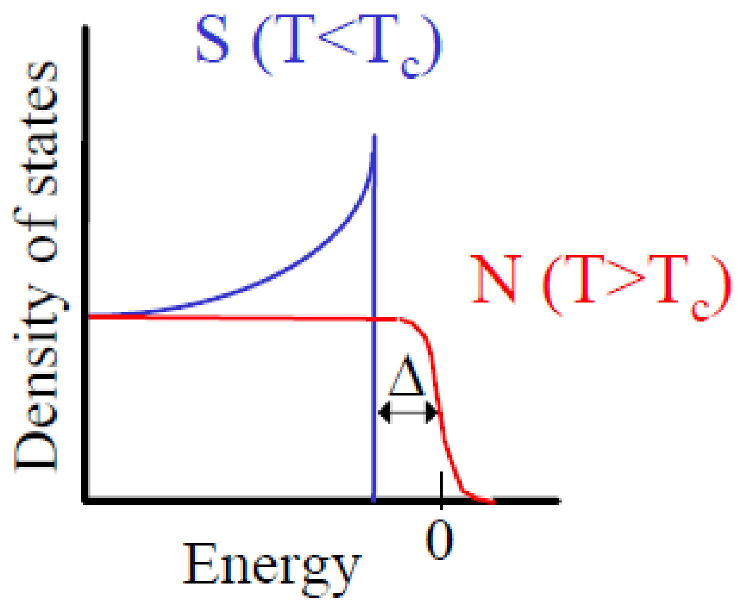

Conventional SCs: T_c~ 0- 30K, Δ ~ 1-2meV

HTSCs: T_c~ 100K, Δ ~ 20-40 meV

超 导 能 隙

Metallic Density of States

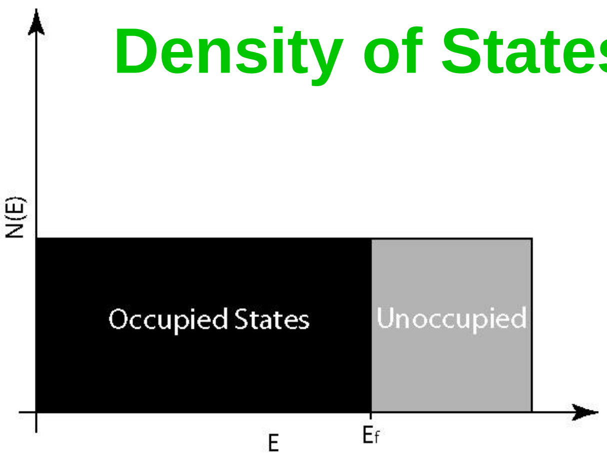

Superconducting Density of States

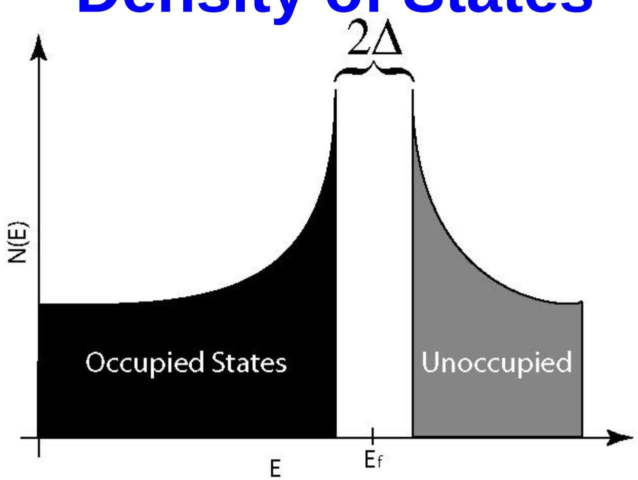

S wave

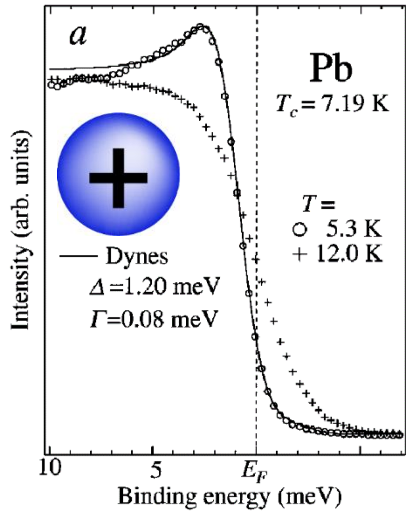

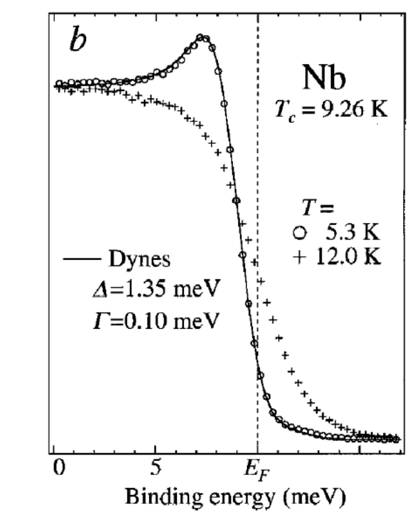

d wave

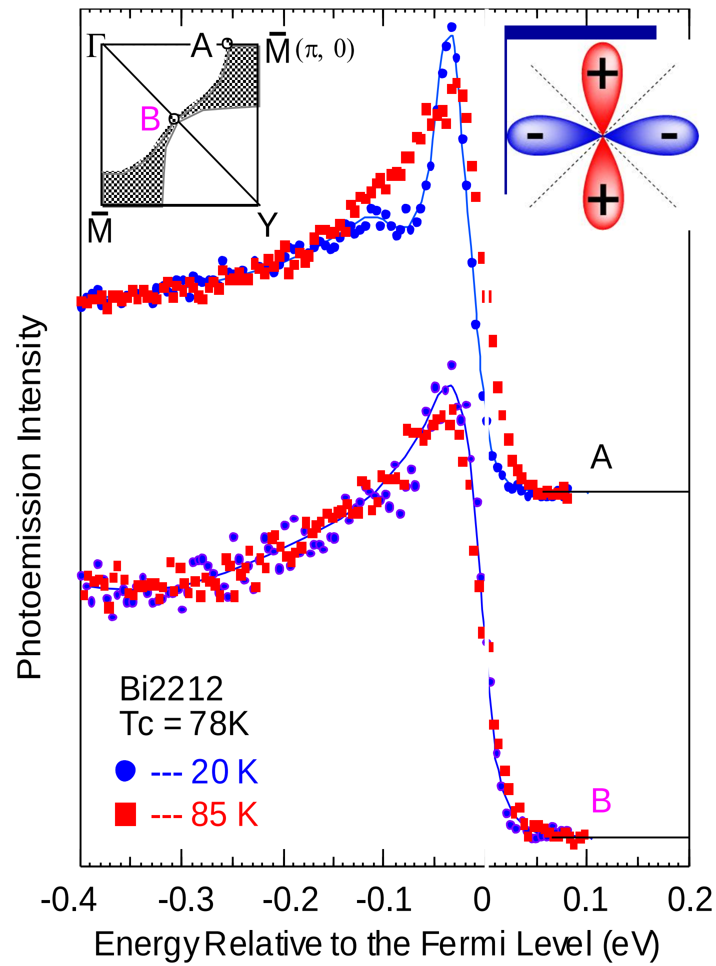

Superconducting order parameter symmetry

SC gap ? = magnitude of order parameter. Varies as a function of k in a d-wave SC

$$\frac{\Psi(r1,\sigma1;r2,\sigma2)=\psi(\text{orbital})\cdot\chi(\text{spin})}{\text{Antisymmetric under exchange}}$$

χ(spin) : known to be a singlet (S=0) ↓↑

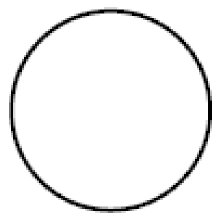

S = 0, l = 0
-- s-wave superconductor
(conventional SC)

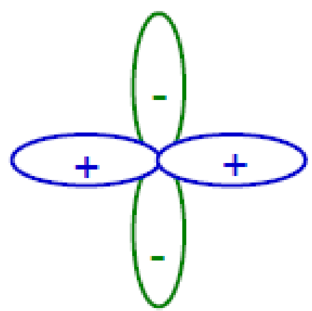

S = 0, l = 2
-- d-wave superconductor
(HTSCs - pretty sure)

Hole-like Fermi Surface

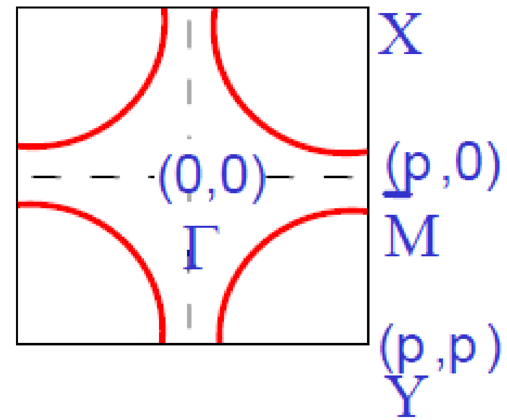

d-wave SC gap - maximal near (p,0)

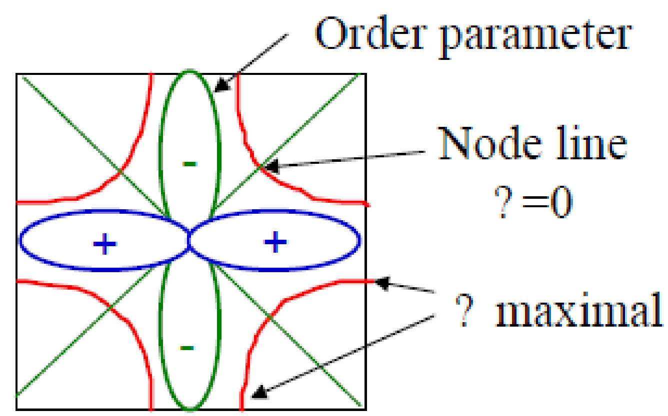

Z-X Shen, D.S. Dessau et al,
PRL **70**, 1553 (1993).

EDC 和 MDC

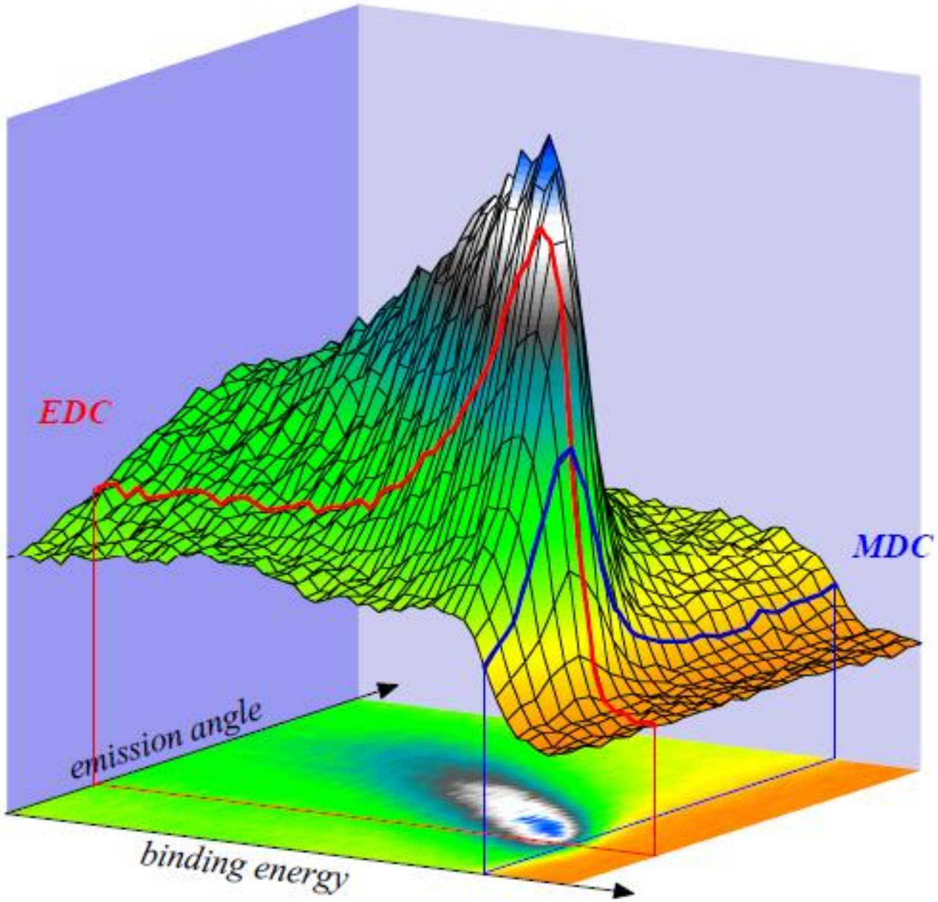
EDC
MDC
emission angle
binding energy

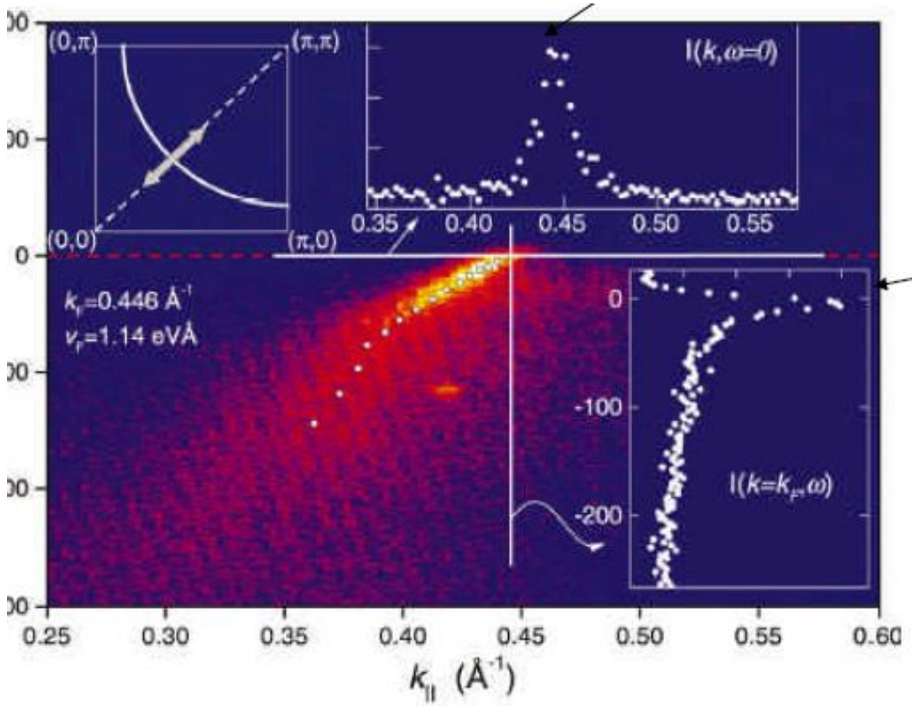
(0,π)
(π,π)
(0,0)
(π,0)
I(k,ω=0)
0.35
0.40
0.45
0.50
0.55
k_F=0.446 Å^{-1}
v_F=1.14 eVÅ
0
-100
-200
I(k=k_F,ω)
0.25
0.30
0.35
0.40
0.45
0.50
0.55
0.60
$k_{||}$ (Å^{-1})

Early gap measurements on HTSCs

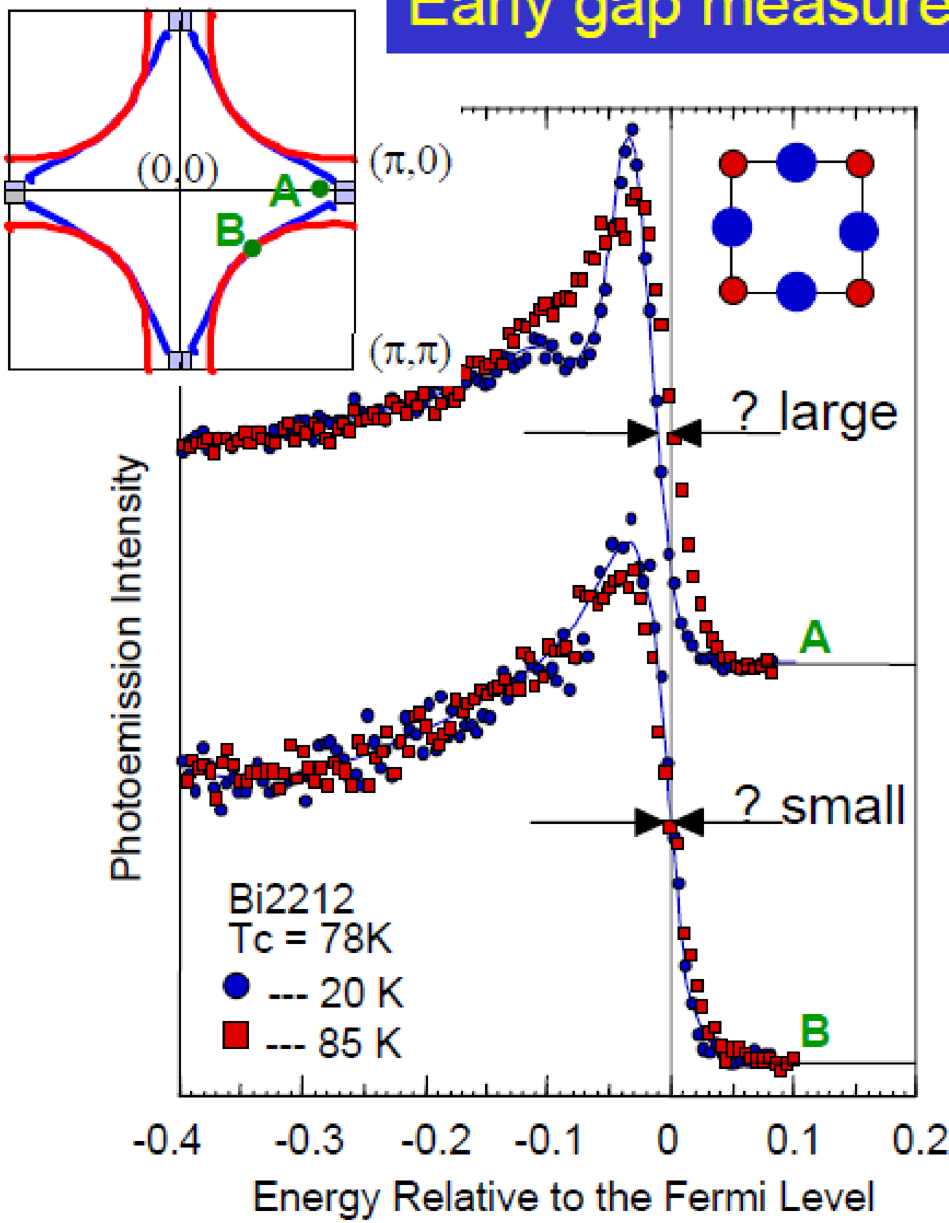

Gap magnitude maximal at (p,0), minimal or zero along (0,0)-(p,p) "nodal line."
--> $d_{x^2-y^2}$ symmetry order parameter

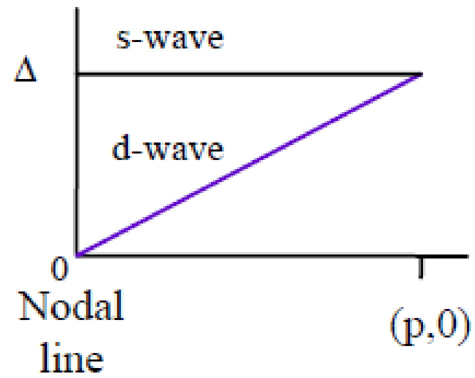

Famous peak-dip-hump structure at (p,0).
--> interaction with some mode?

Z.-X. Shen, D.S. Dessau et al., Phys. Rev. Lett. **70** 1553 (1993)

PHYSICAL REVIEW B VOLUME 54, NUMBER 14 1 OCTOBER 1996-II

Angle-resolved photoemission spectroscopy study of the superconducting gap anisotropy in $Bi_2Sr_2CaCu_2O_{8+x}$

H. Ding, M.R. Norman, J.C. Campuzano, et al.

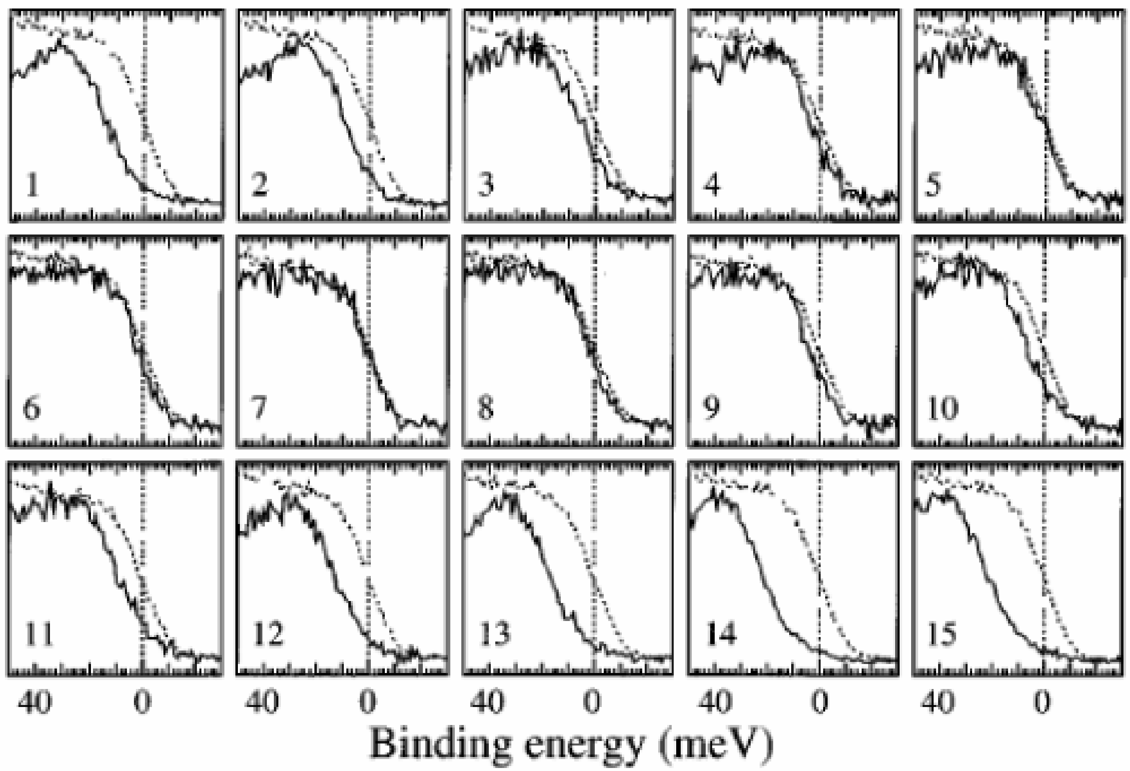

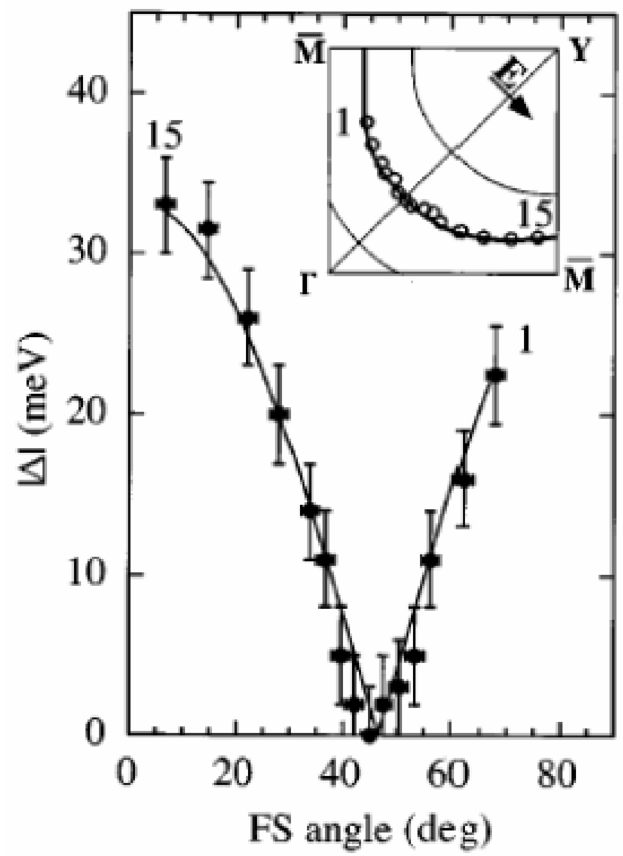

Gap and Pseudogap

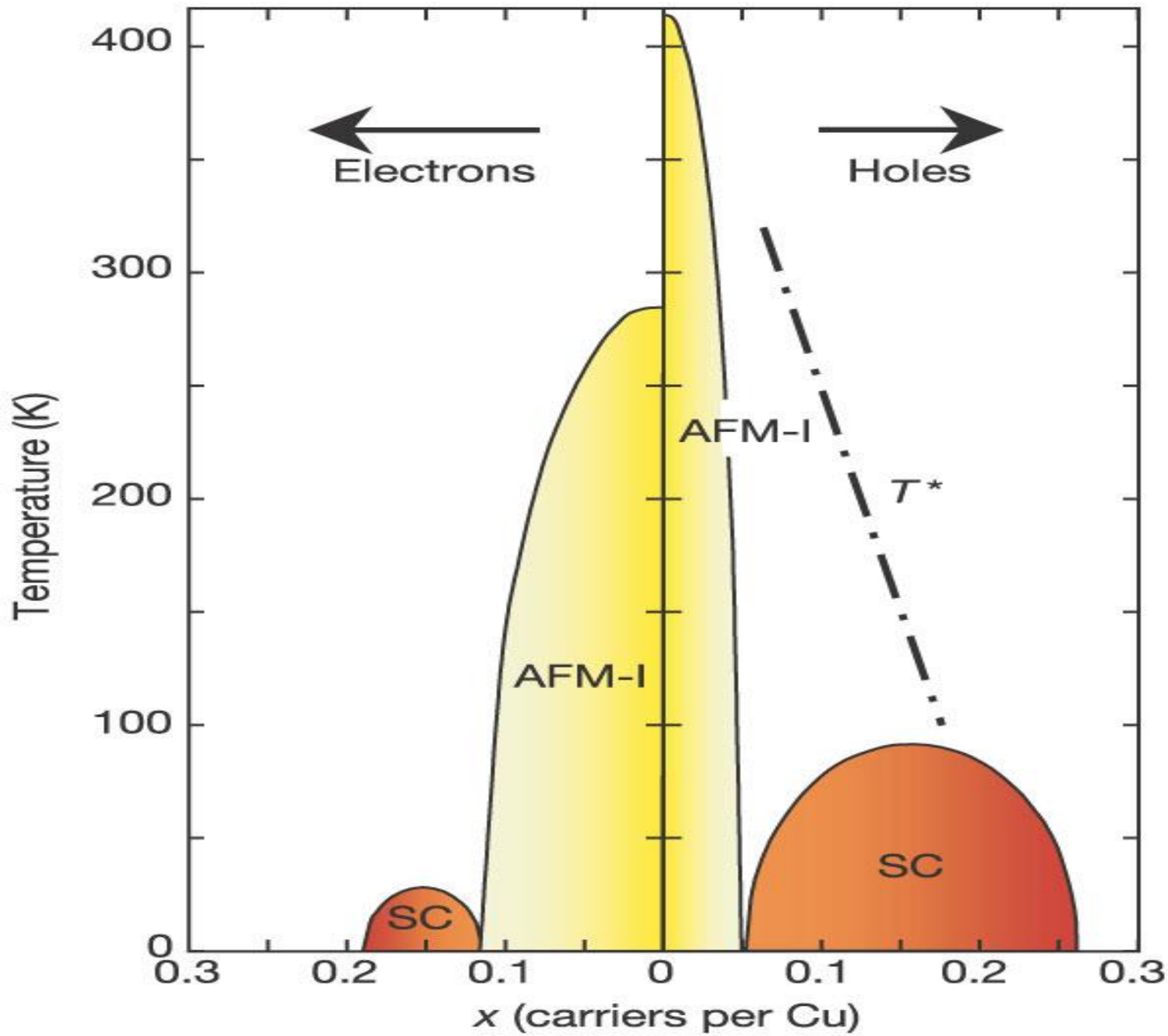

Spectroscopic evidence for a pseudogap in the normal state of underdoped high T_C superconductors

*H. Ding et al. Nature **382**, 51 (1996).*

antinode

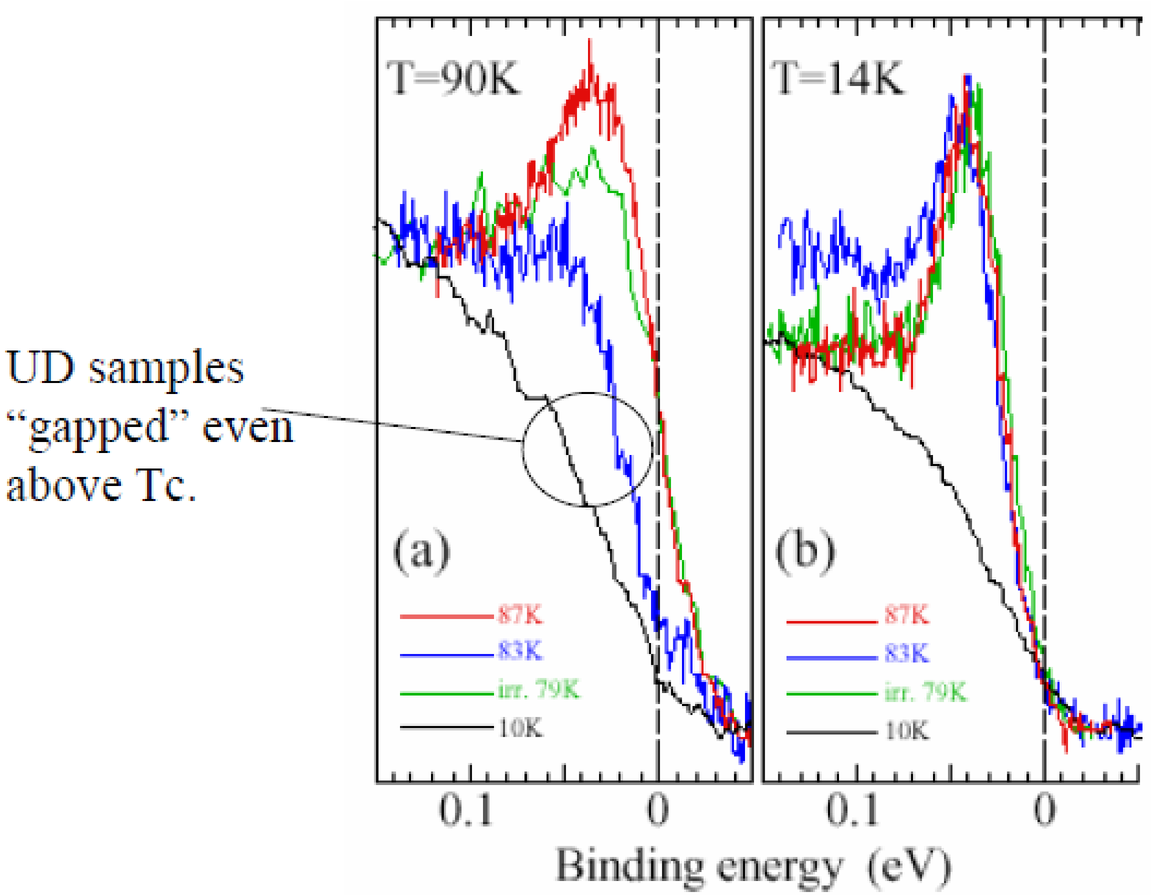

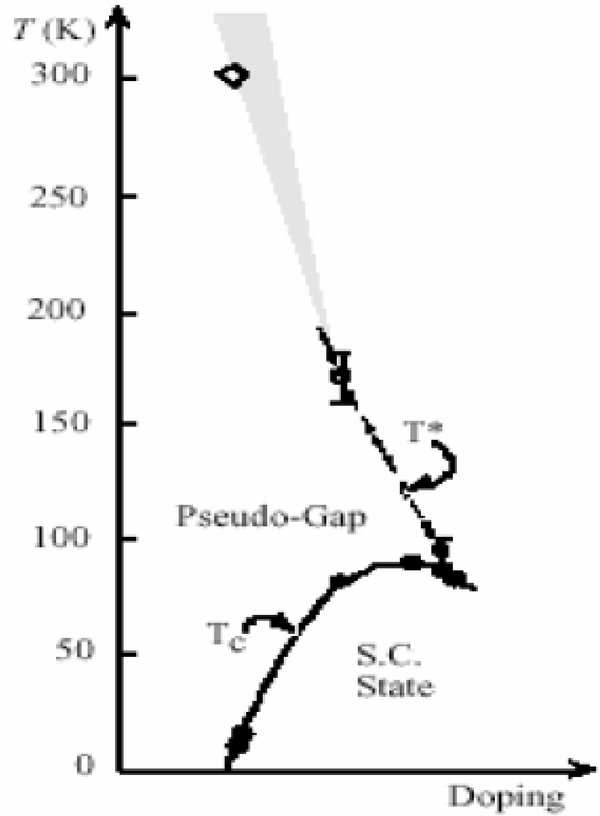

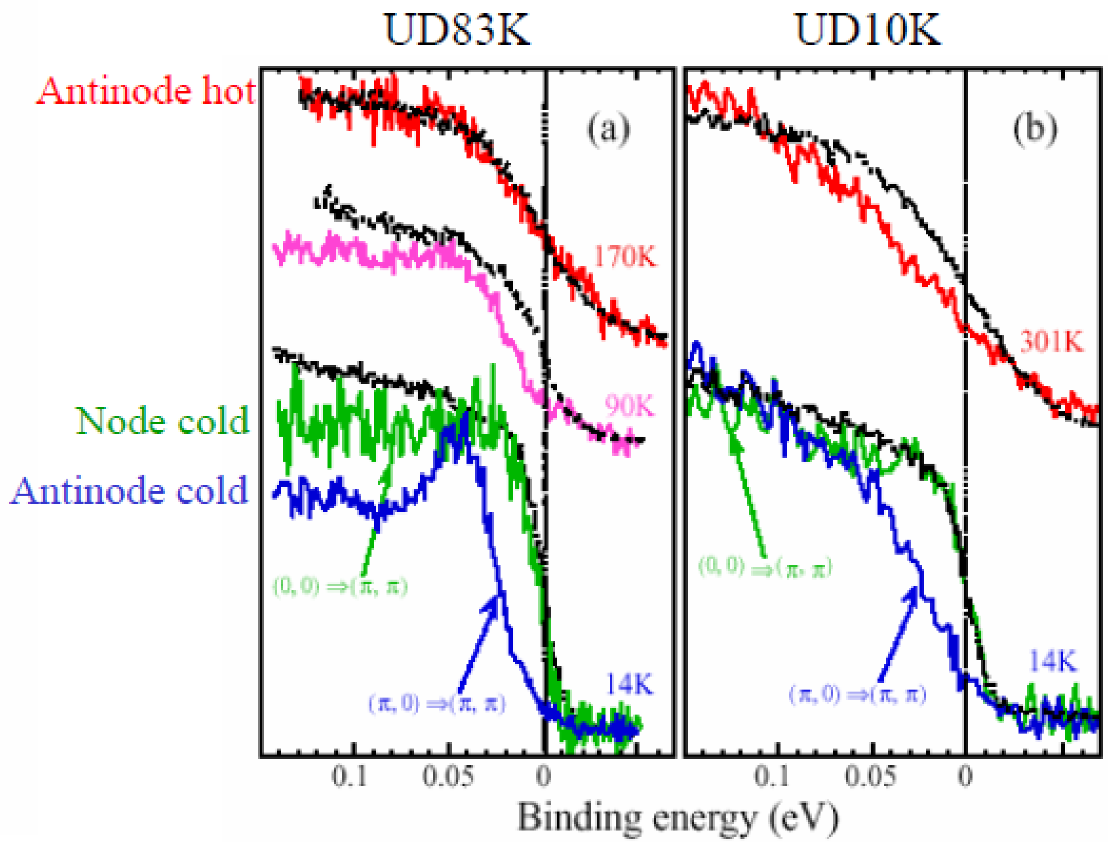

Thought to exist between Tc and T* for UD samples.
Similar magnitude as SC gap.
Similar k-dependence as SC gap (d-wave).
Obtained from leading edge analysis.

Also
*M. Norman et al, Nature **392**, 157(1998).*
*D.S. Marshall et al, PRL **76**, 4841 (1996).*
*A.G. Loeser et al. Science **273**, 325 (1996).*

判定能隙与赝能隙的方法

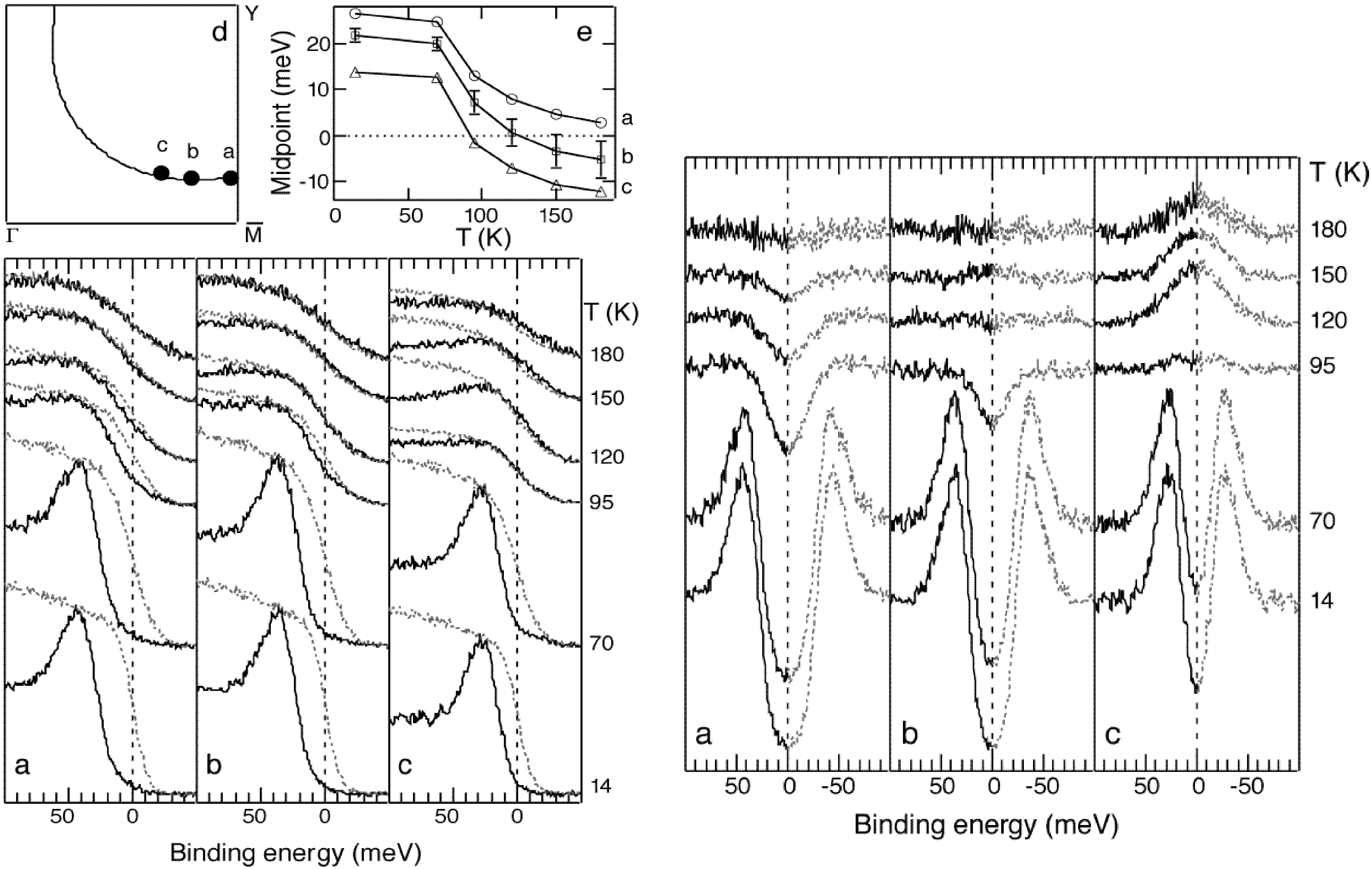

Two-gap electronic structure

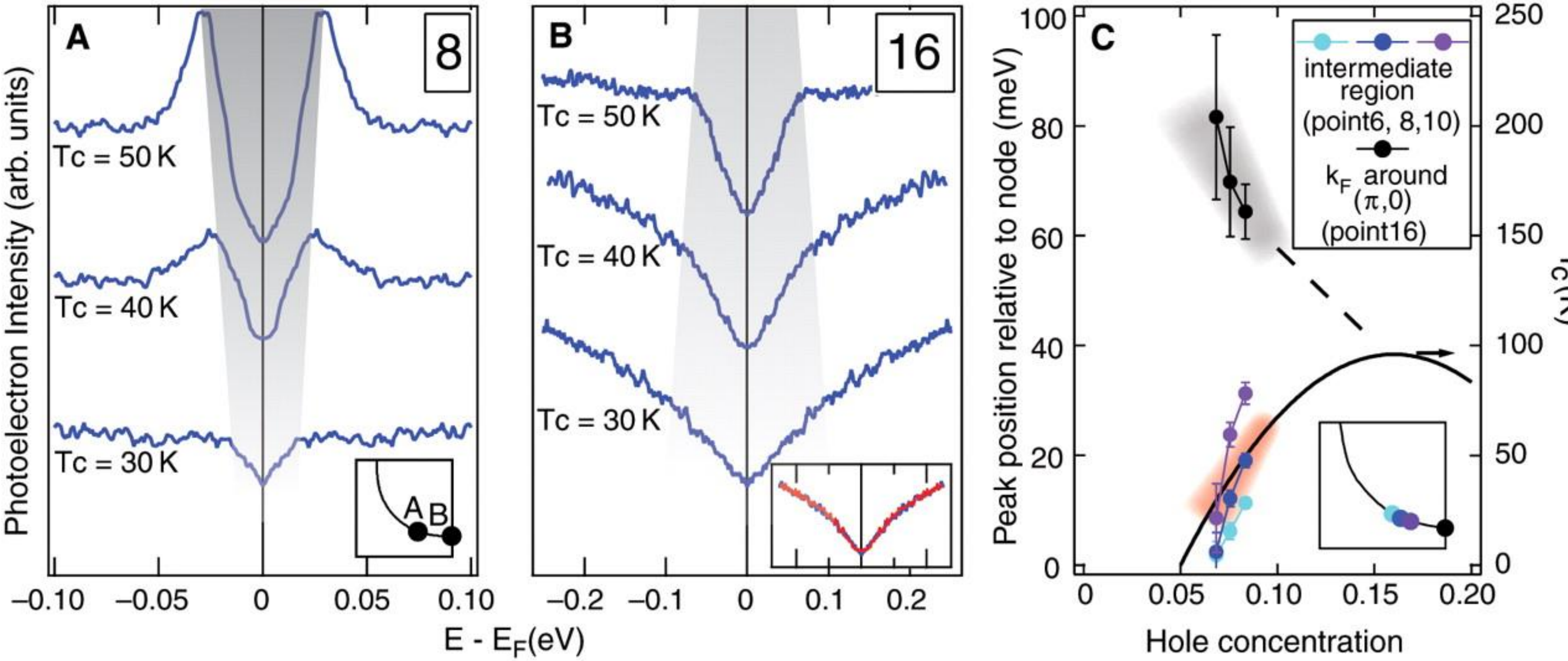

Nodal 能隙

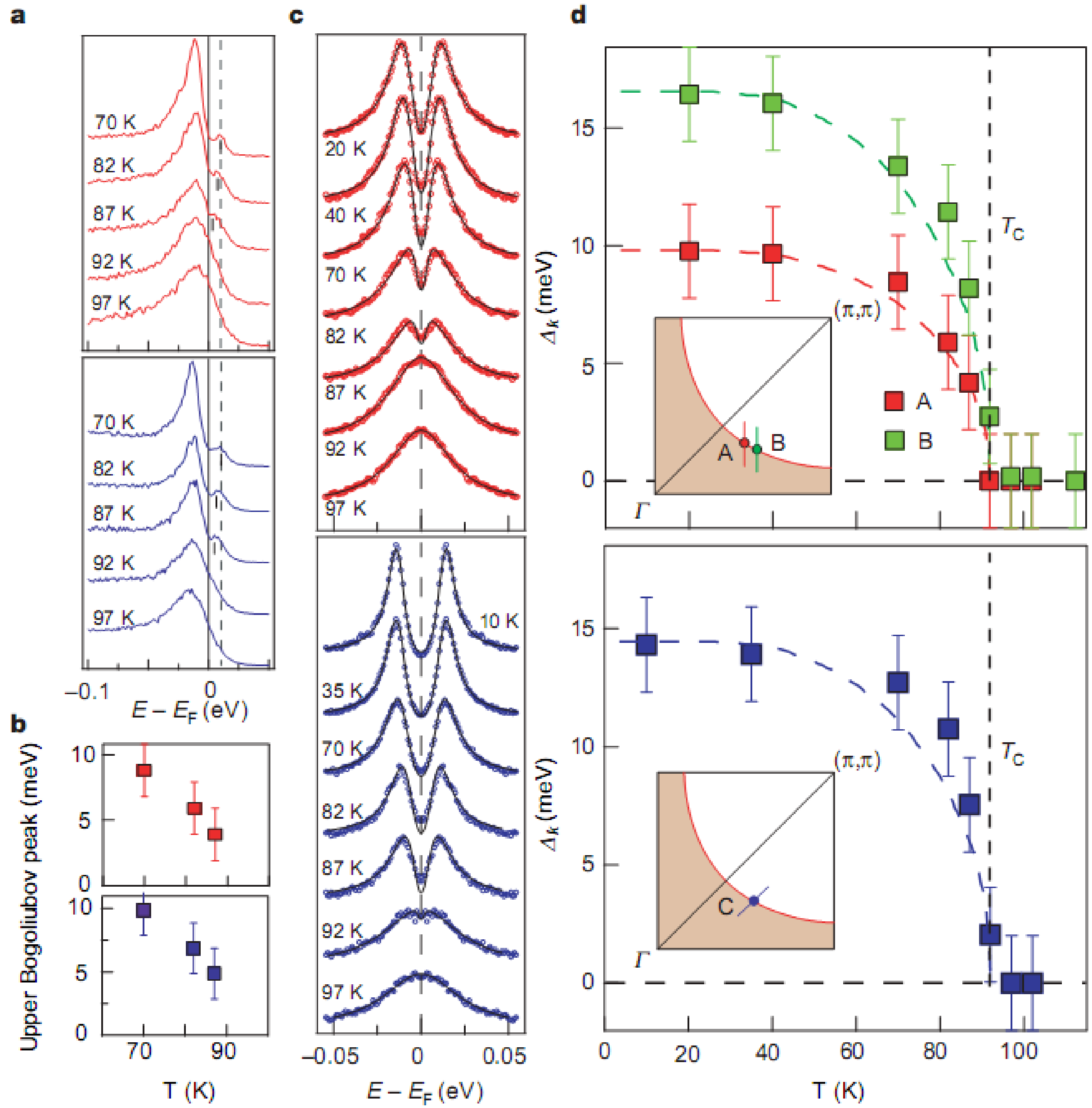

a
70 K
82 K
87 K
92 K
97 K
70 K
82 K
87 K
92 K
97 K
−0.1
0
E − E_F (eV)
b
Upper Bogoliubov peak (meV)
10
5
0
10
5
0
70
90
T (K)
c
20 K
40 K
70 K
82 K
87 K
92 K
97 K
10 K
35 K
70 K
82 K
87 K
92 K
97 K
−0.05
0
0.05
E − E_F (eV)
d
15
10
5
0
Δ_k (meV)
T_c
(π,π)
A
B
Γ
A
B
15
10
5
0
Δ_k (meV)
T_c
(π,π)
C
Γ
0
20
40
60
80
100
T (K)

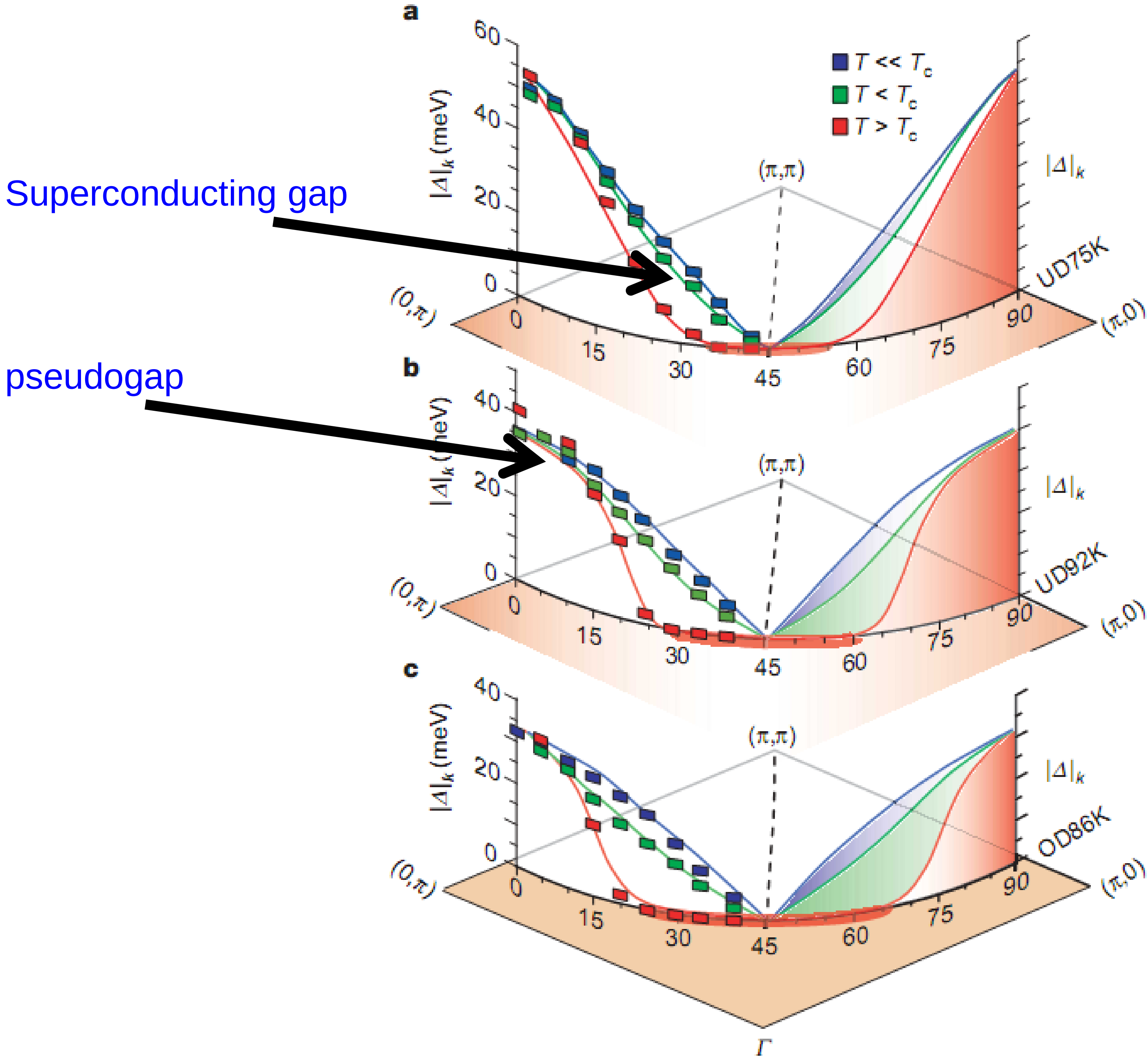

Superconducting gap
pseudogap
a
b
c
$T << T_c$
$T < T_c$
$T > T_c$
$|\Delta|_k$ (meV)
$|\Delta|_k$
(π,π)
(0,π)
(π,0)
UD75K
UD92K
OD86K
Γ

Creating the ARPES Tunneling Spectrum (ATS)

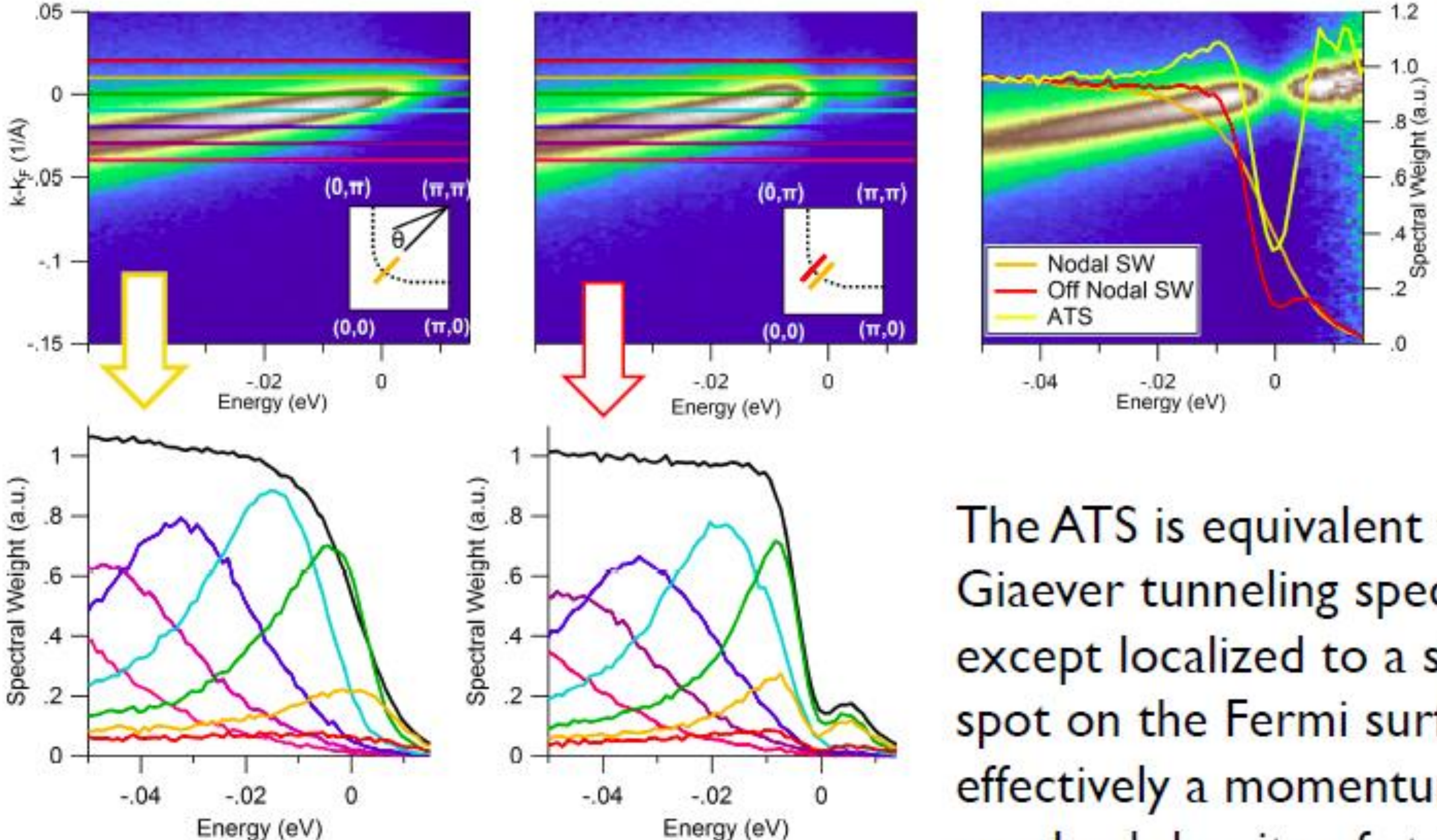

Sample: Bi2212

T: 50 K

T_C: 91 K

hν:7 eV

The ATS is equivalent to a Giaever tunneling spectrum except localized to a single spot on the Fermi surface, effectively a momentum resolved density of states.

Onnes

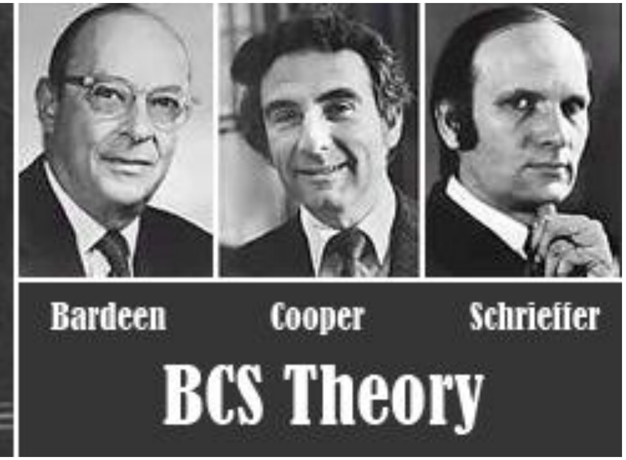

缪勒和贝德诺尔茨

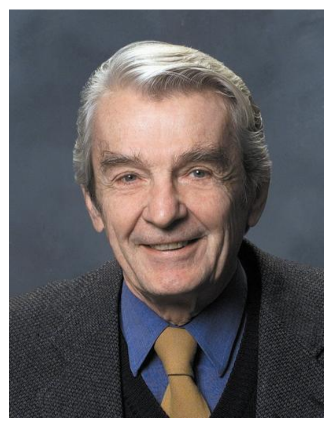

Giaver

Brian D. Josephson

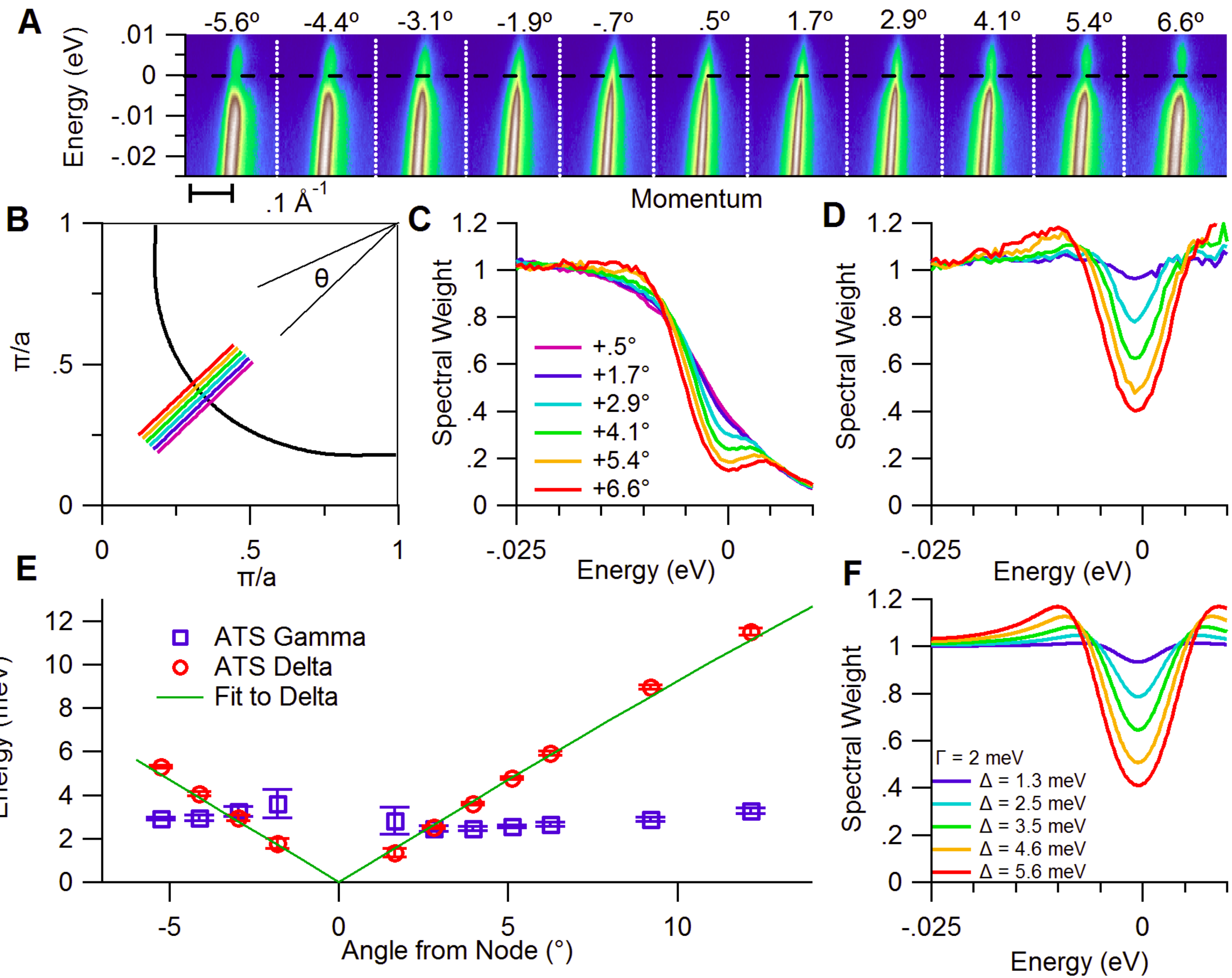
A
-5.6°
-4.4°
-3.1°
-1.9°
-.7°
.5°
1.7°
2.9°
4.1°
5.4°
6.6°
Energy (eV)
.1 Å^{-1}
Momentum
B
π/a
θ
C
Spectral Weight
+.5°
+1.7°
+2.9°
+4.1°
+5.4°
+6.6°
Energy (eV)
D
Spectral Weight
Energy (eV)
E
Energy (meV)
ATS Gamma
ATS Delta
Fit to Delta
Angle from Node (°)
F
Spectral Weight
Γ = 2 meV
Δ = 1.3 meV
Δ = 2.5 meV
Δ = 3.5 meV
Δ = 4.6 meV
Δ = 5.6 meV
Energy (eV)

Comparison to Leading Edge and Symmetrized EDCs

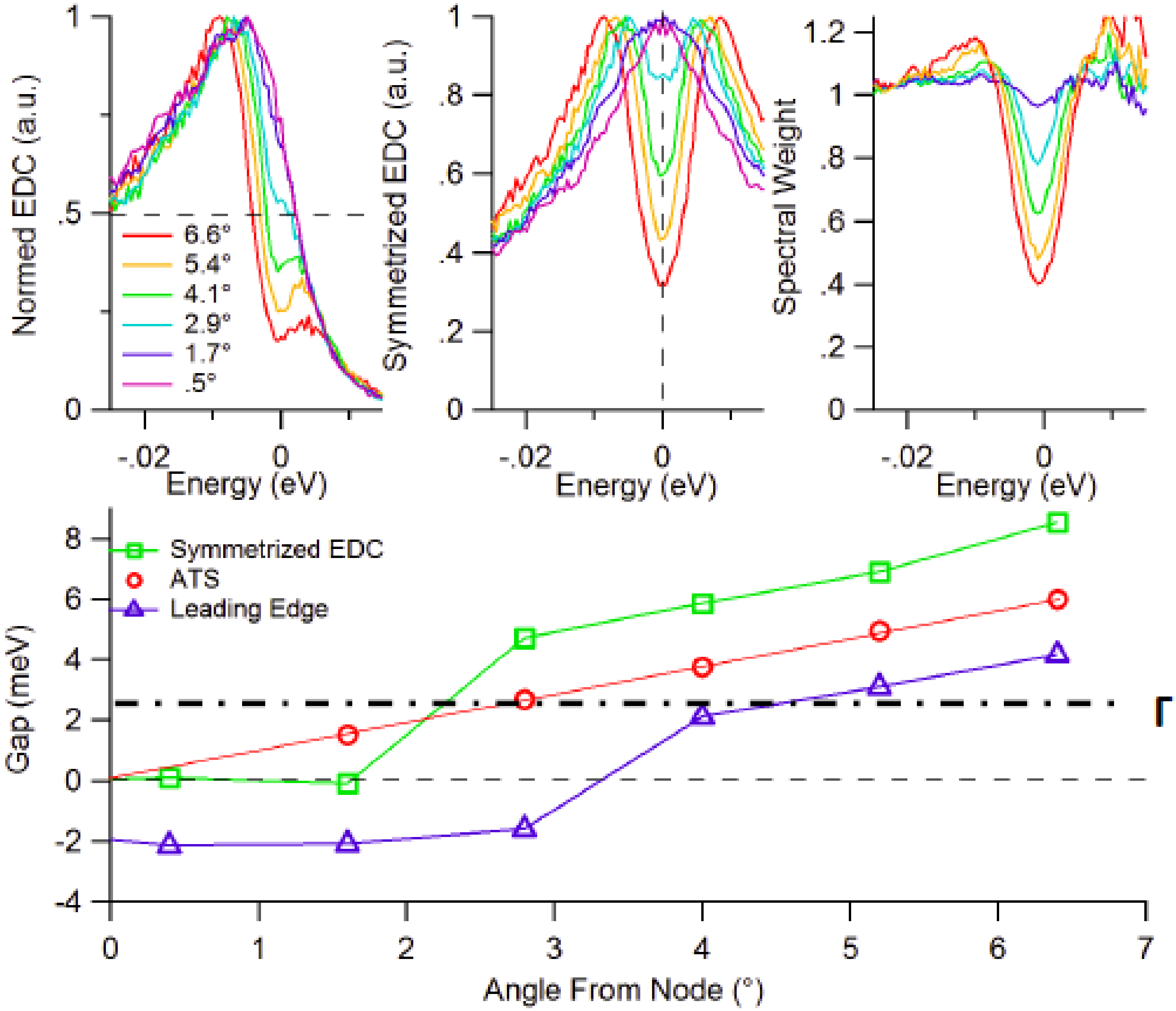

Sample:
Bi2212
T: 50 K
T_C: 91 K
hv:7 eV

Both conventional techniques (Leading Edge and Symmetrized EDCs) result in a finite arc where the gap is zero.

The arc forms when $\Gamma > \Delta$.

电子-玻色子相互作用

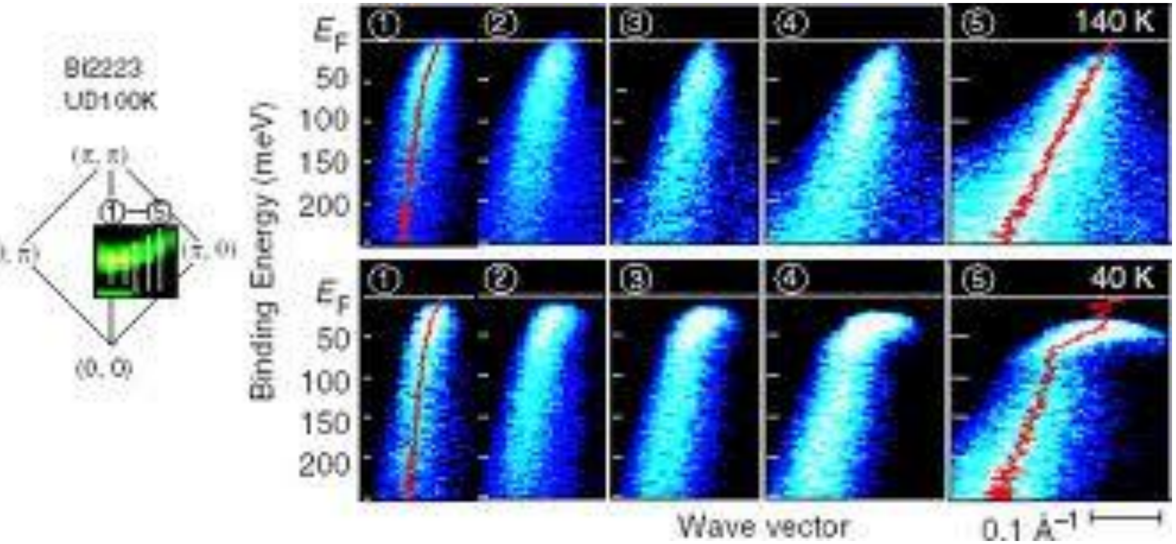

Bi2223
UD100K
(π, π)
(π, 0)
(0, 0)
140 K
40 K
Binding Energy (meV)
Wave vector
0.1 Å⁻¹

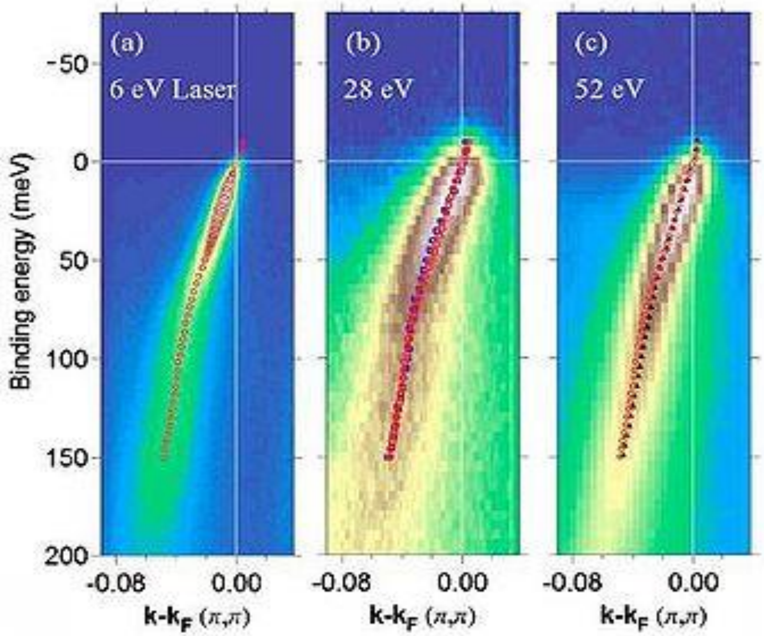

(a)
6 eV Laser
(b)
28 eV
(c)
52 eV
Binding energy (meV)
k-k_F (π,π)

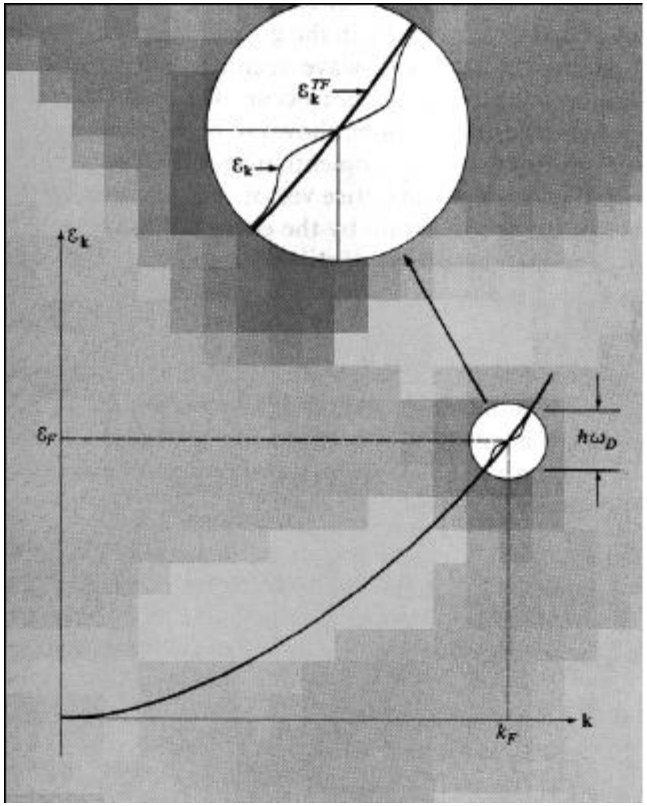

ε_k
ε_F
k_F
k
ħω_D

Stanford Group
Lanzara et al.
Nature **412**,510 (2001)

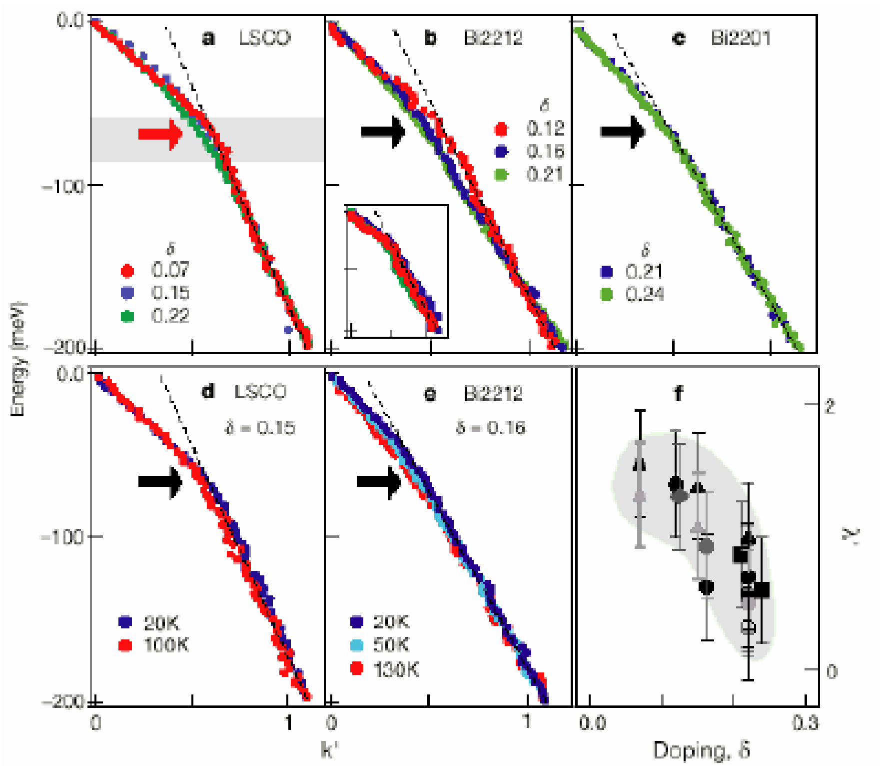

Brookhaven Group
Johnson et al.
cond-mat/0102260 (2001).

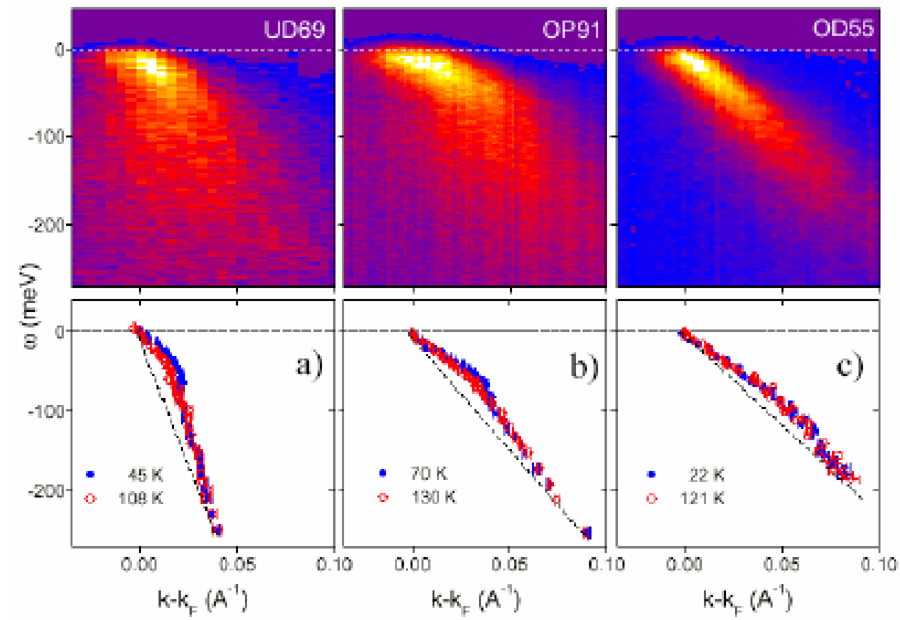

Argonne Group
Kaminski et al.
PRL **86**, 1070 (2001)

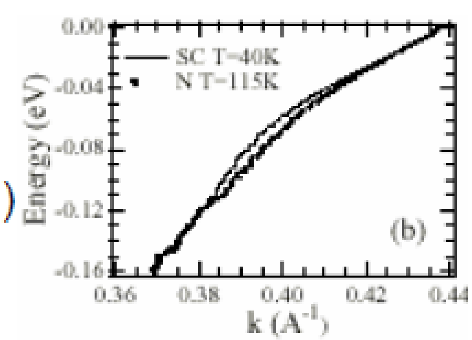

$Bi_2Sr_2CaCu_2O_8$的氧同位素效应

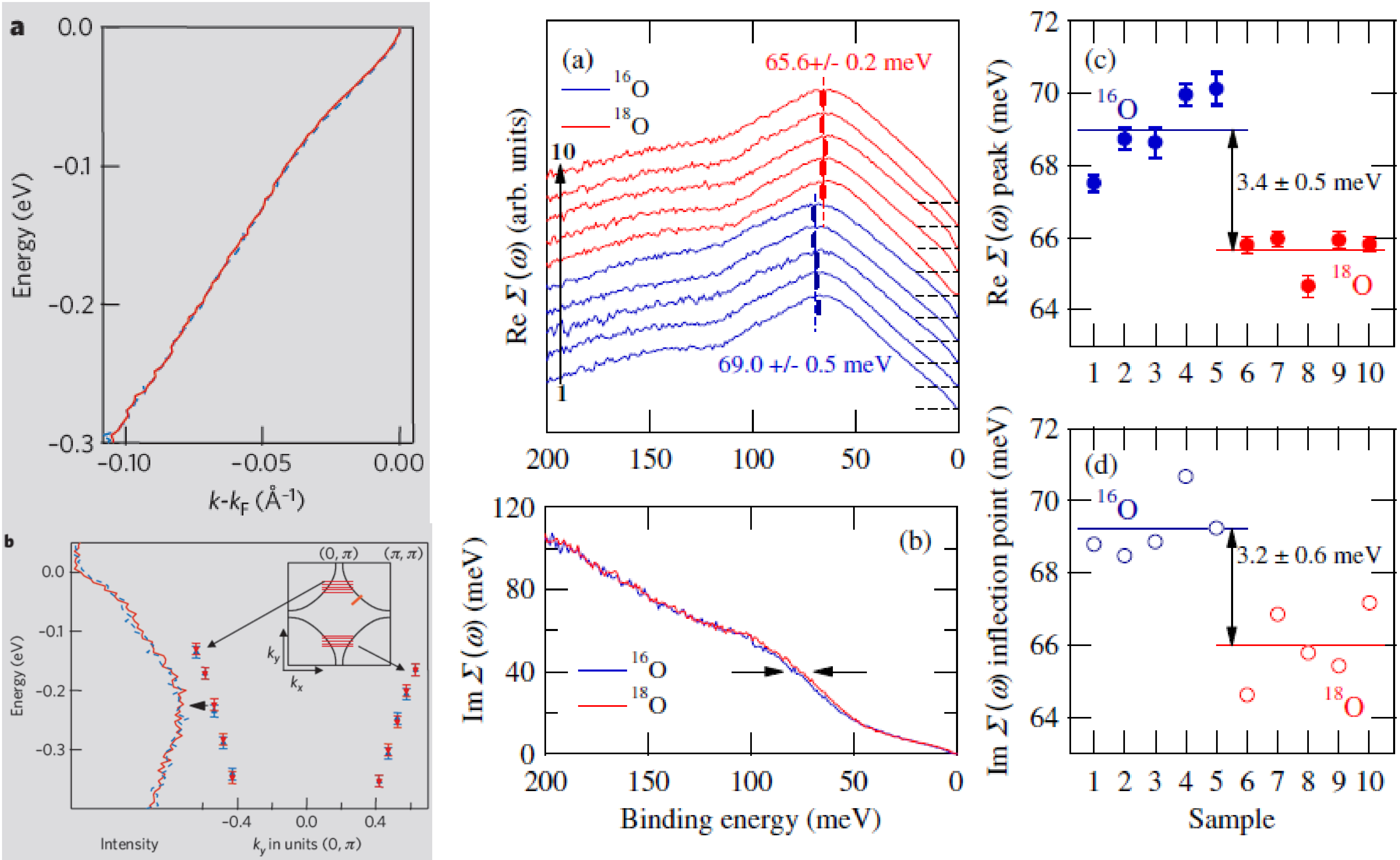

H. Iwasawa

$Bi_2Sr_2CaCu_2O_8$的超精细低能能带结构

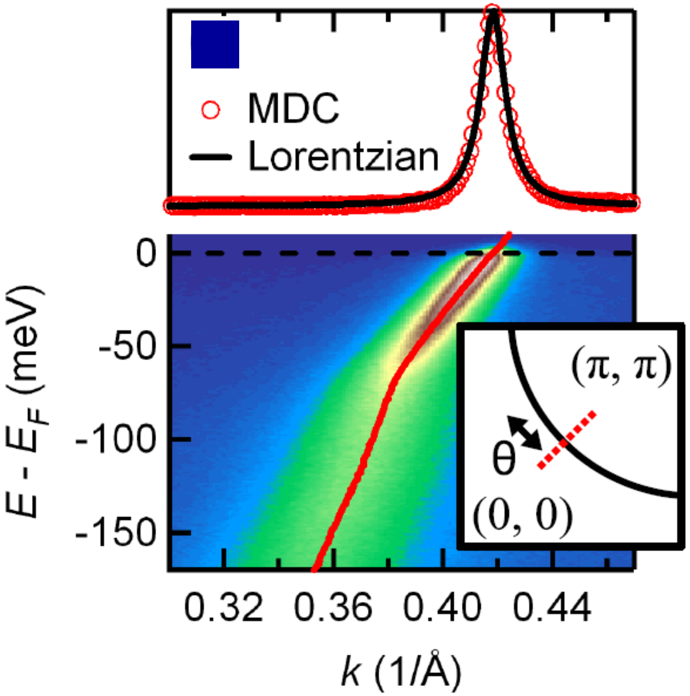

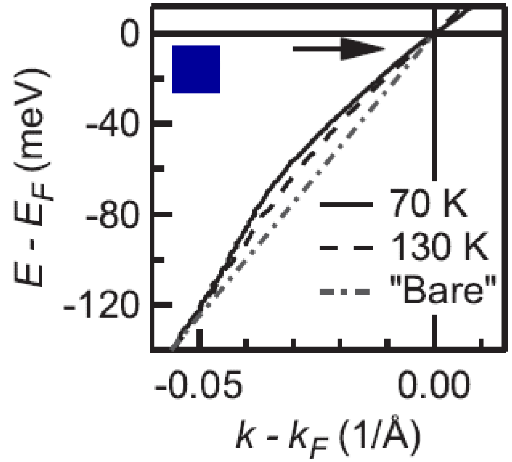

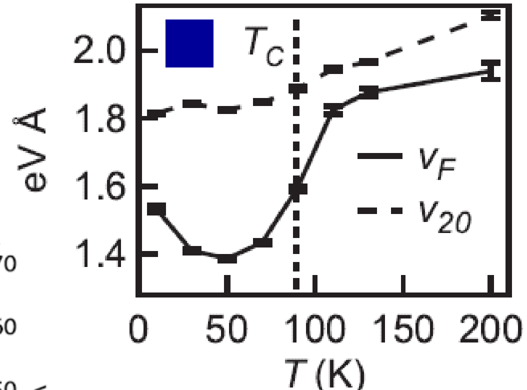

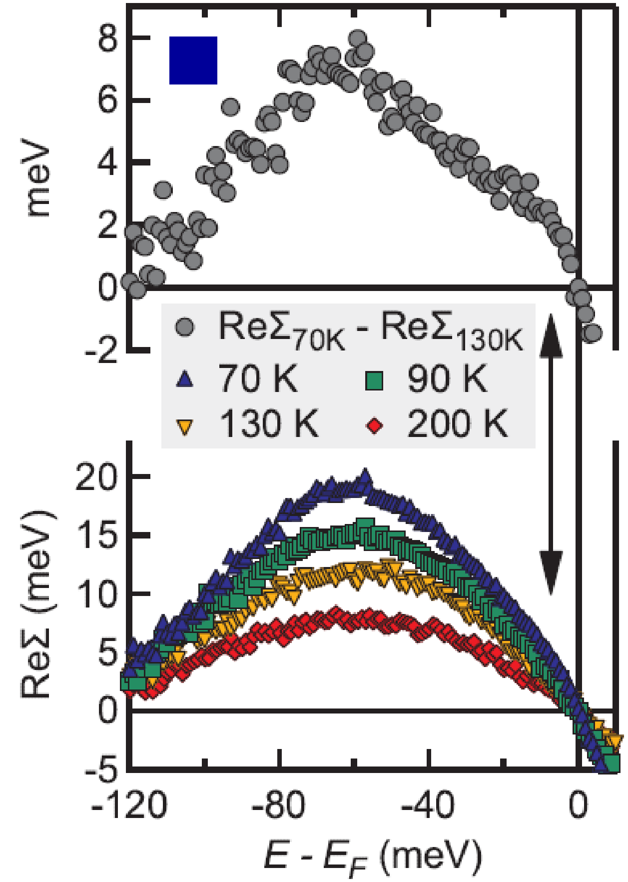

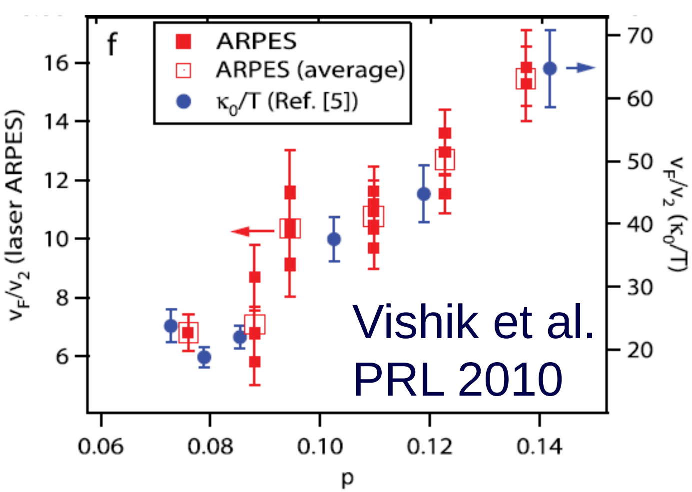

低能能带结构对输运的贡献
可以在热导数据中显示出来。

Nick Plumb

Richardson-Lucy deconvolution

Superconductivity in the vicinity of AFM

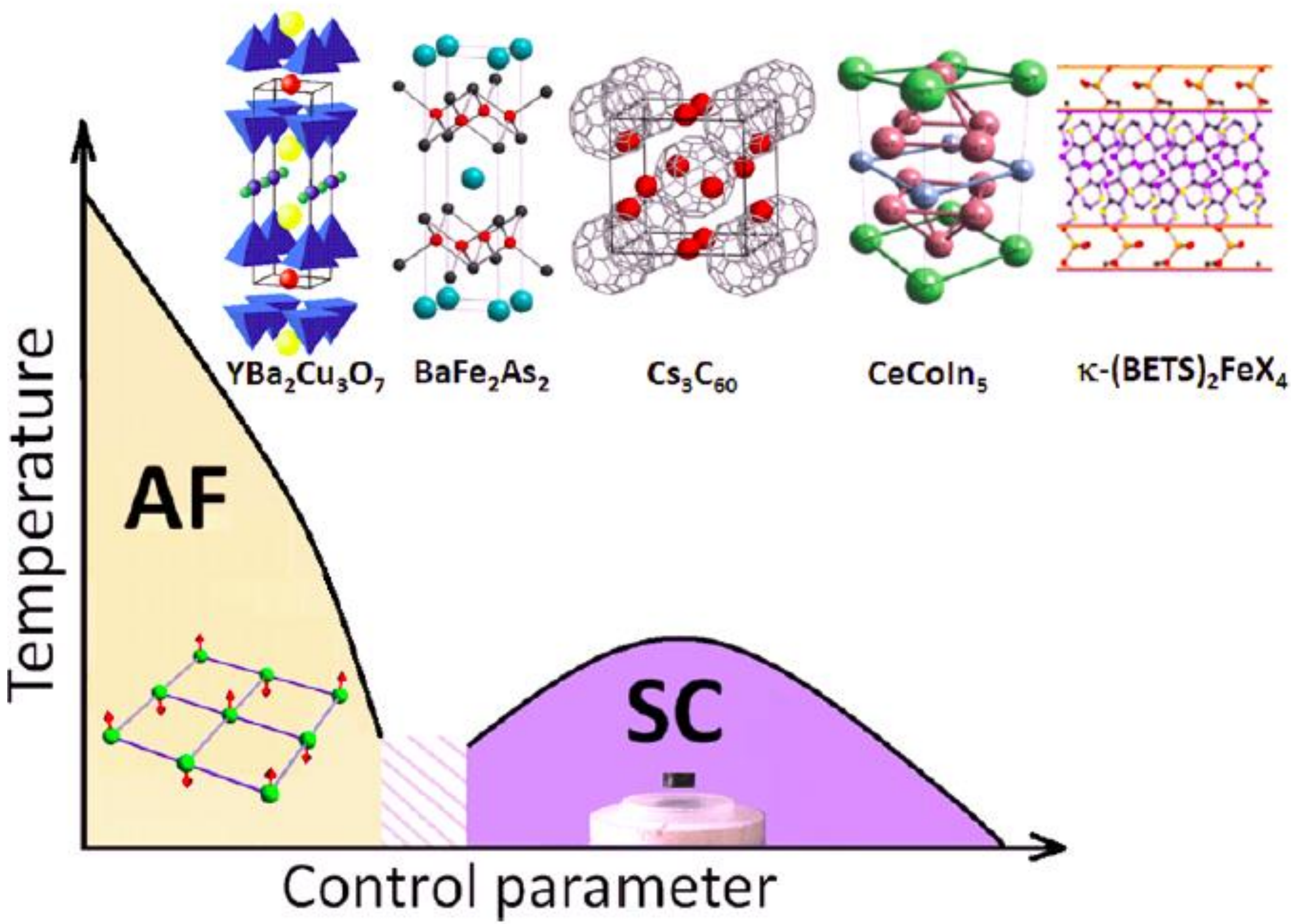

The iron-based materials

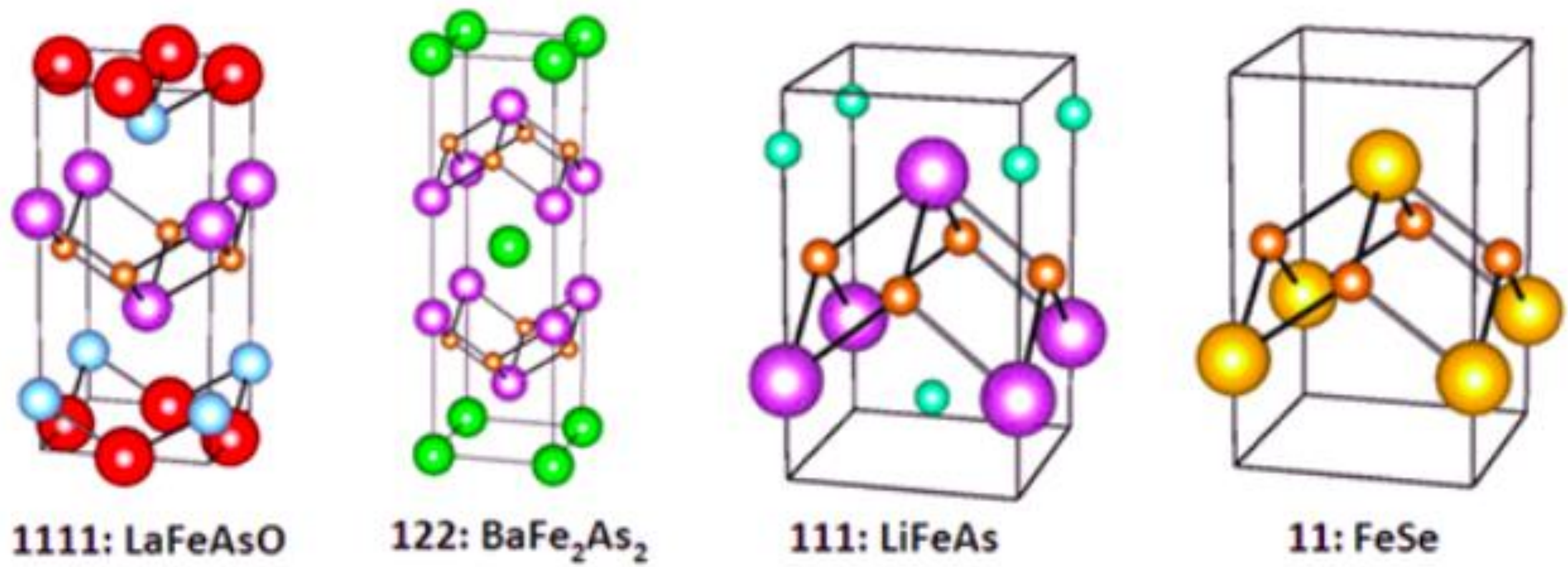

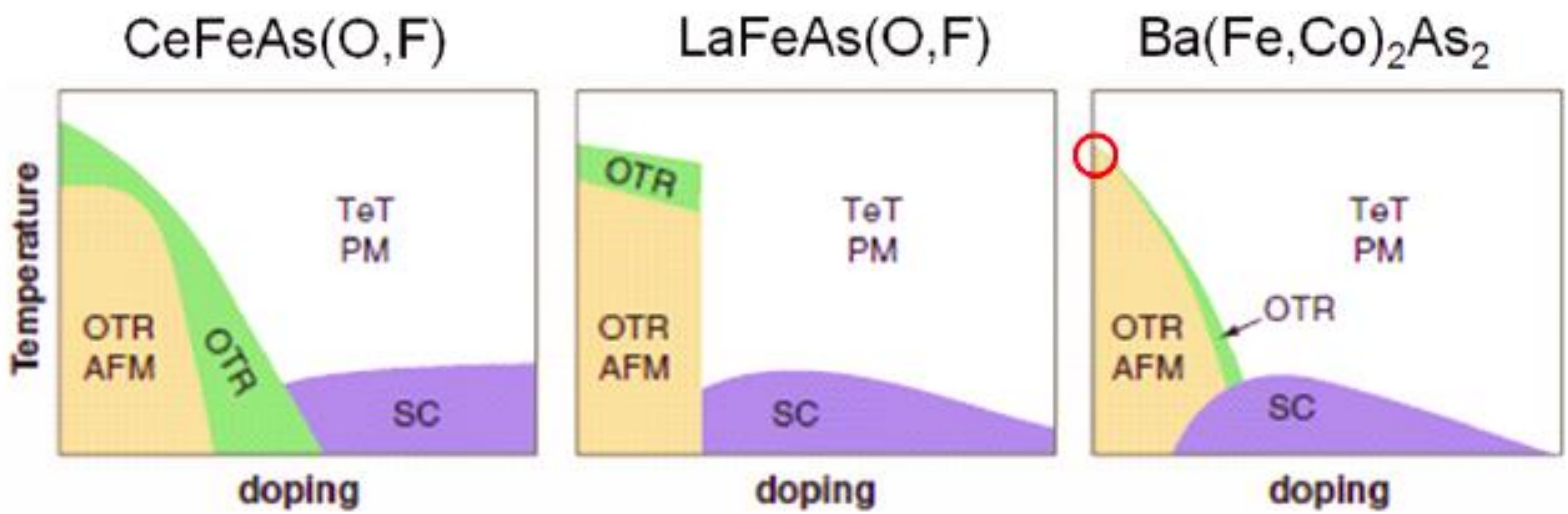

LaFePO – LDA Calculations

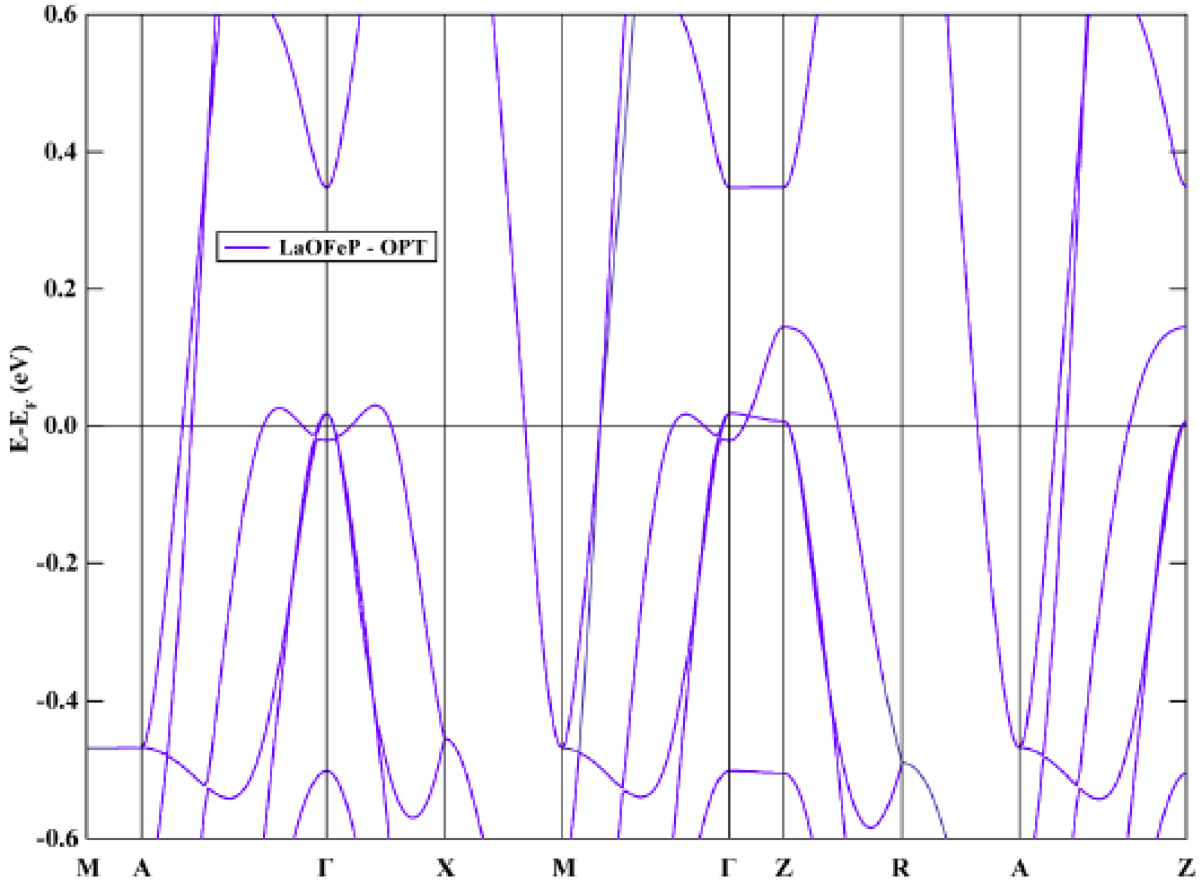

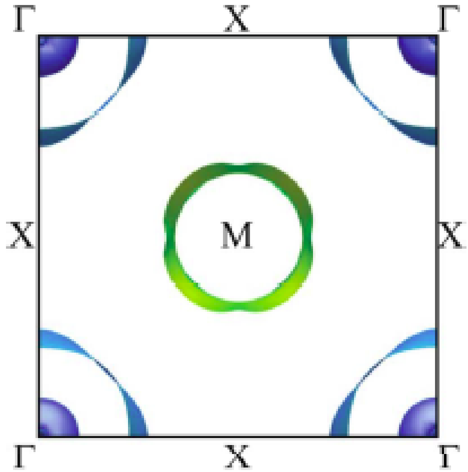

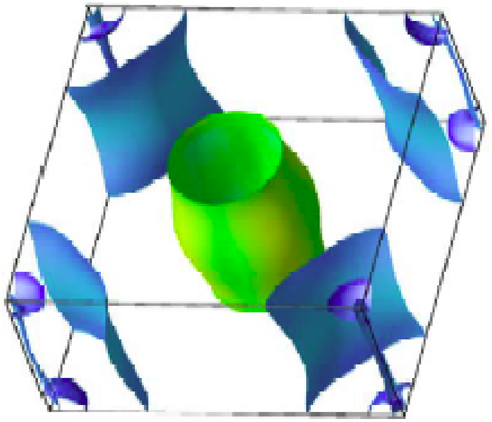

- 5 bands crosses E_F
- 2 electron pockets at M, 3 hole pockets around Γ

Band renormalization

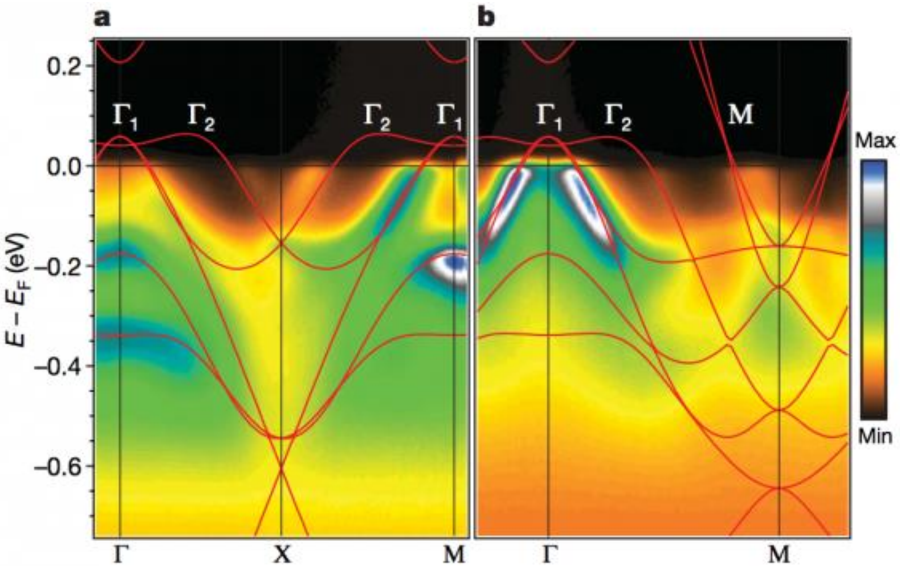

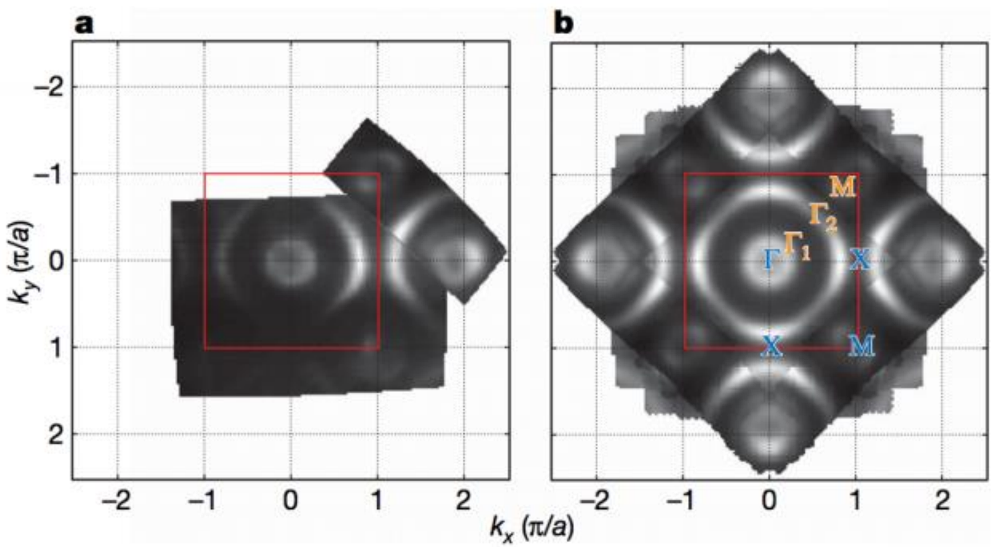

费米面与超导能隙

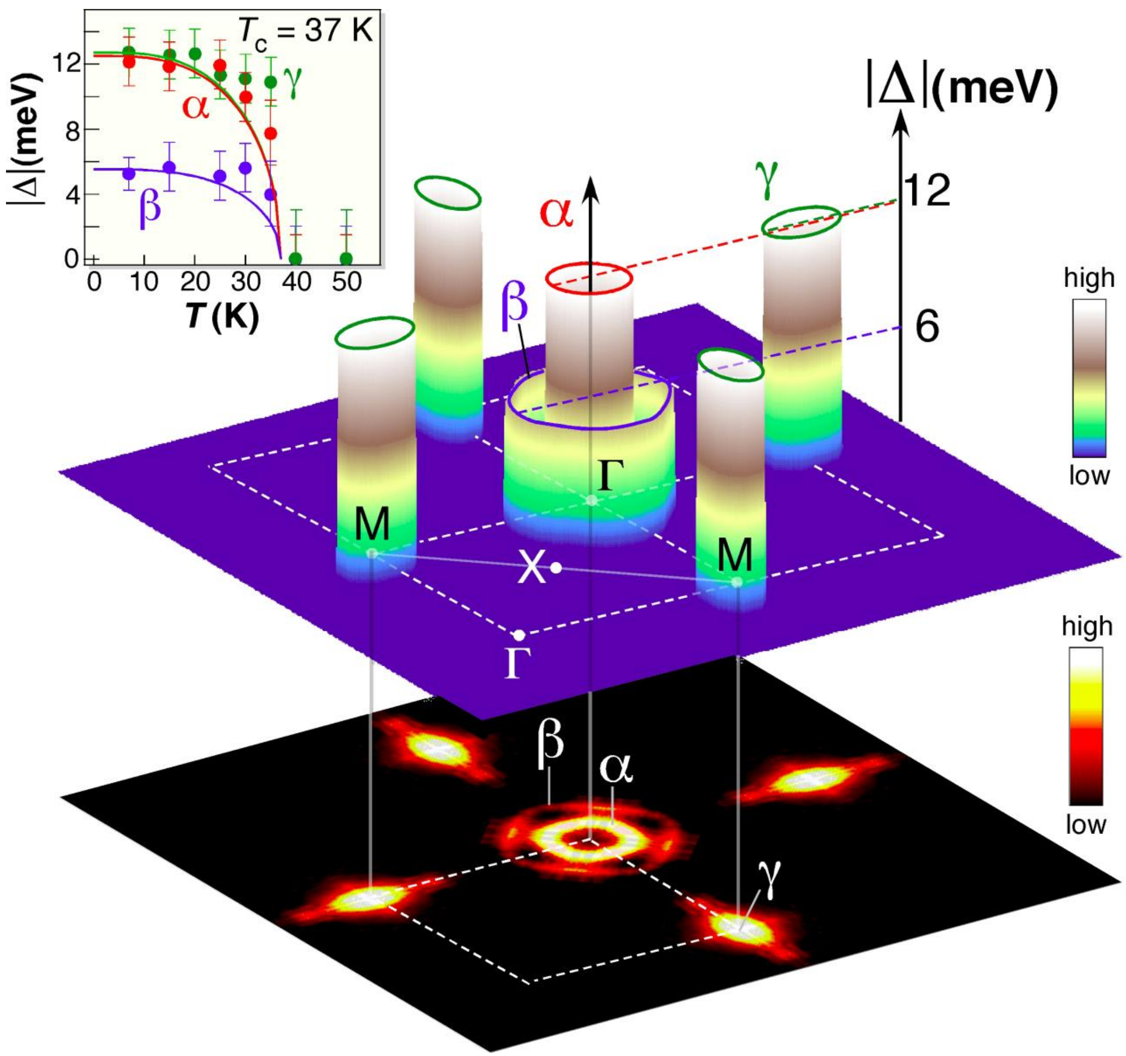

T_c = 37 K
|Δ|(meV)
12
8
4
0
0 10 20 30 40 50
T (K)
α
β
γ
|Δ|(meV)
12
6
α
β
γ
high
low
Γ
M
X
M
Γ
β
α
γ
high
low

超导配对机制

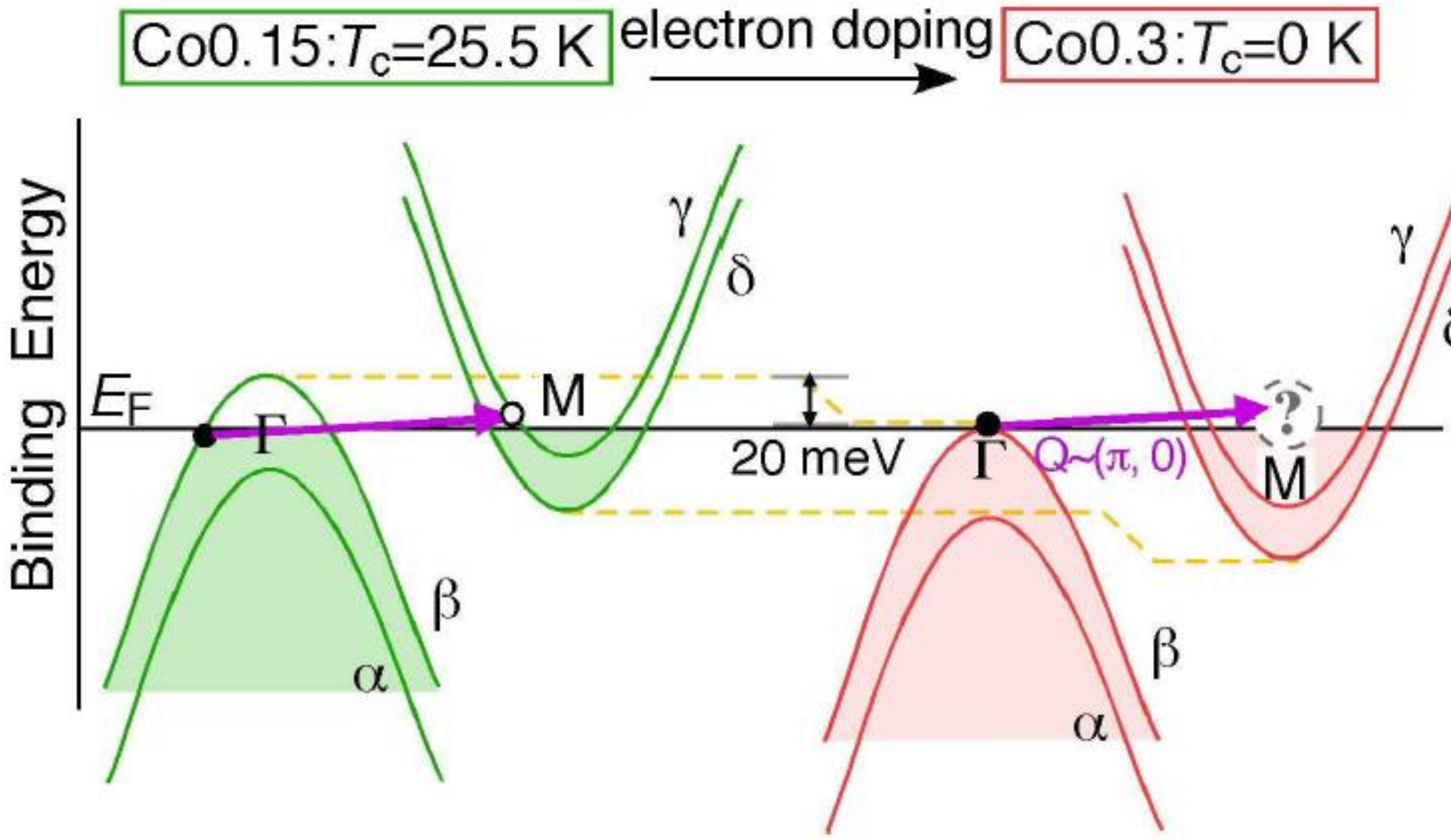

Co0.15:T_c=25.5 K
electron doping
Co0.3:T_c=0 K
Binding Energy
E_F
Γ
M
γ
δ
20 meV
Q~(π, 0)
β
α

Broken symmetry in the orbital degree of freedom

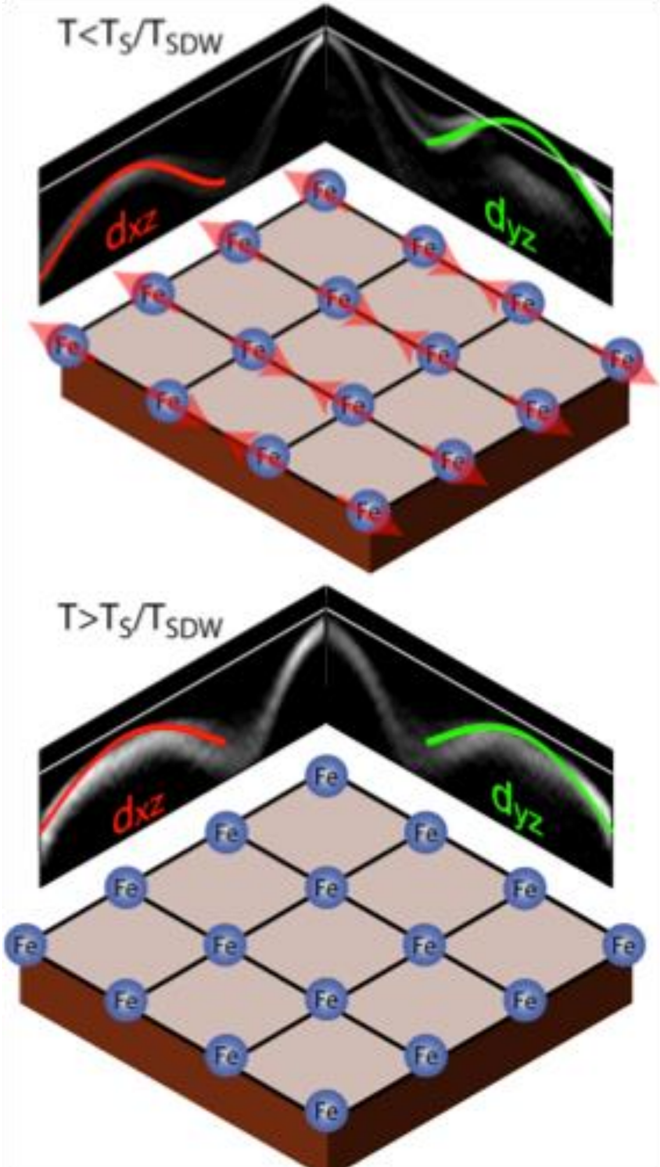

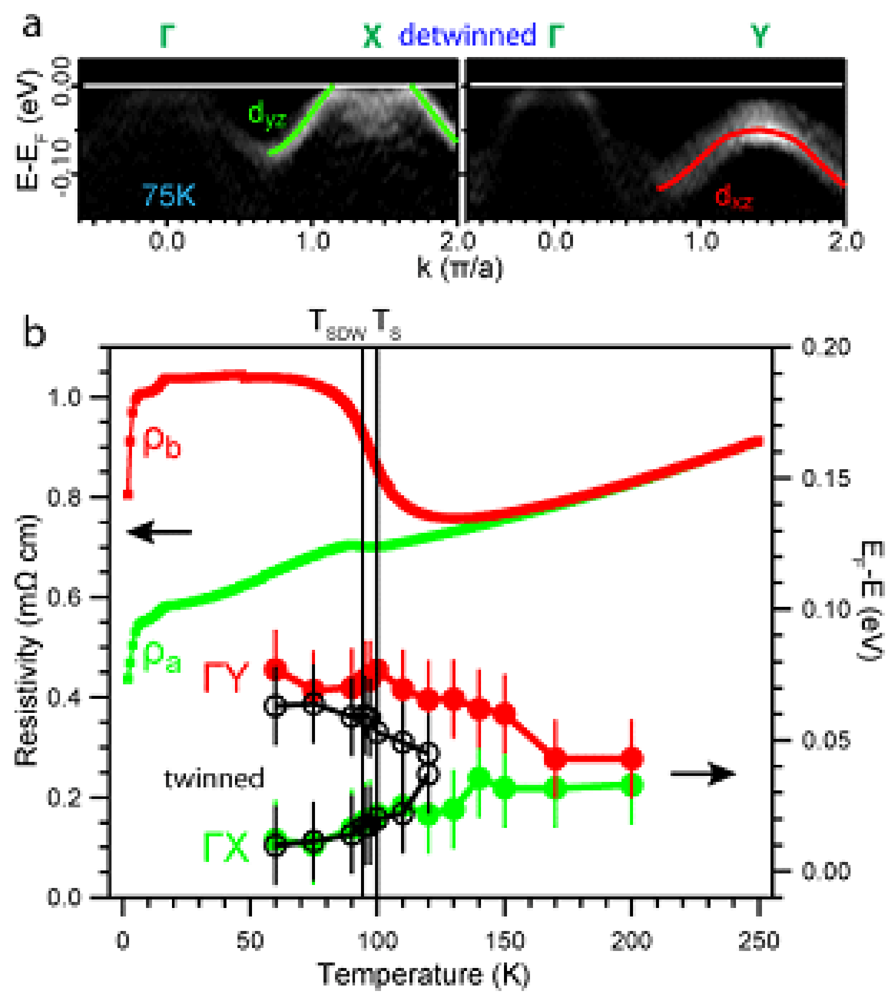

$Ba(Fe_{1-x}Co_x)_2As_2$

Band structure of $K_{0.8}Fe2Se2$

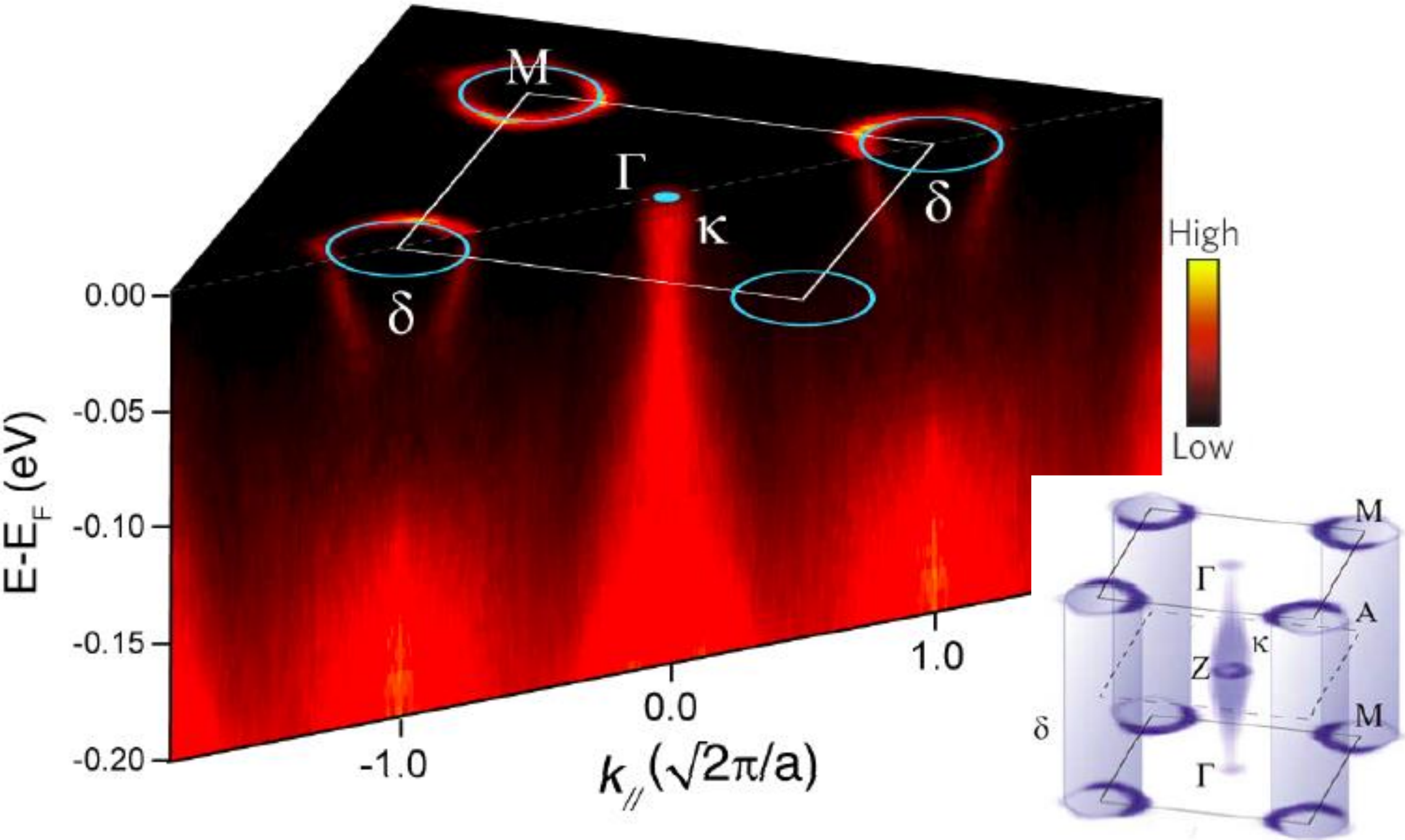

Feng group

Band structure and Gaps

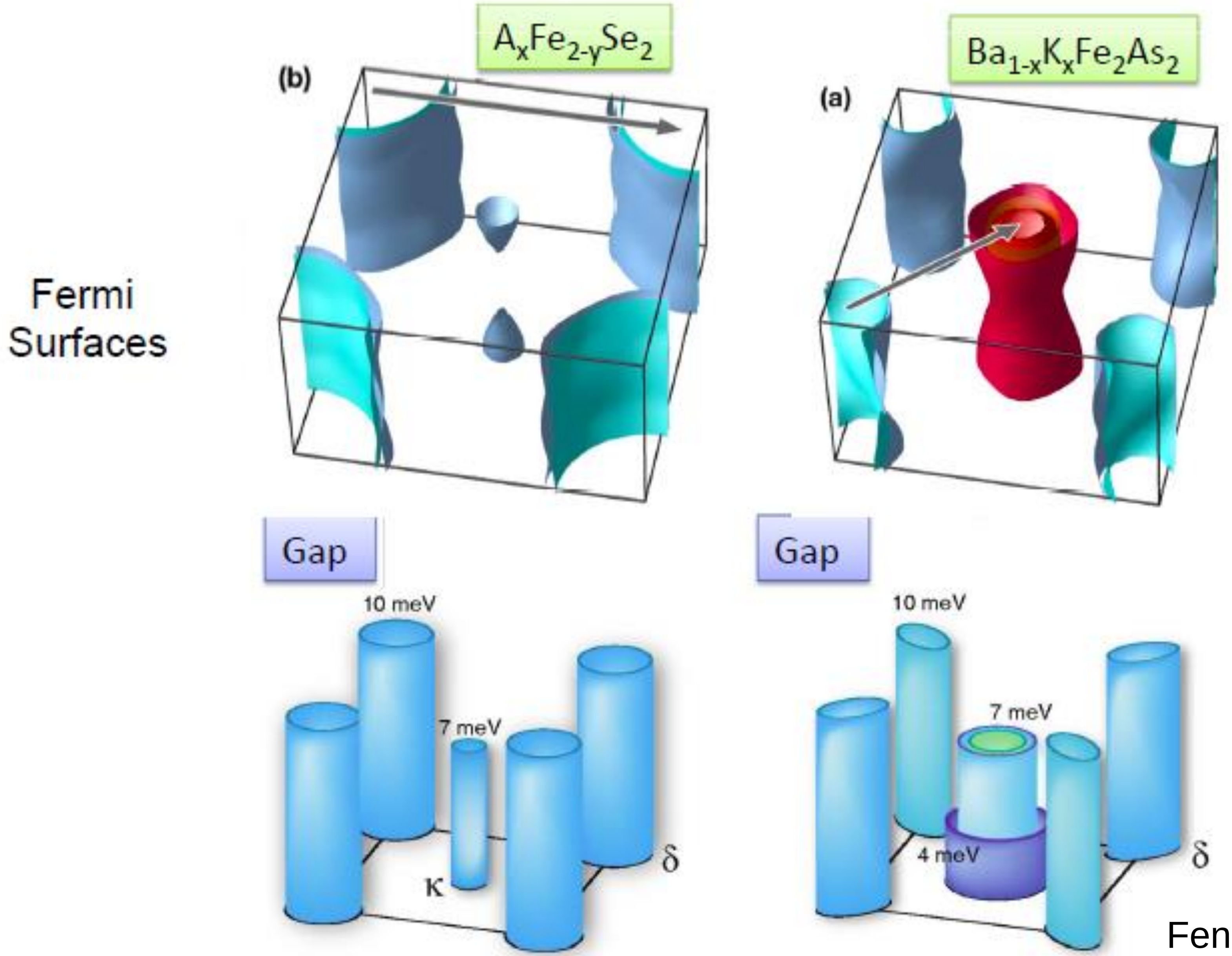

Feng group

Phase diagram of $K_xFe_{2-y}Se_2$

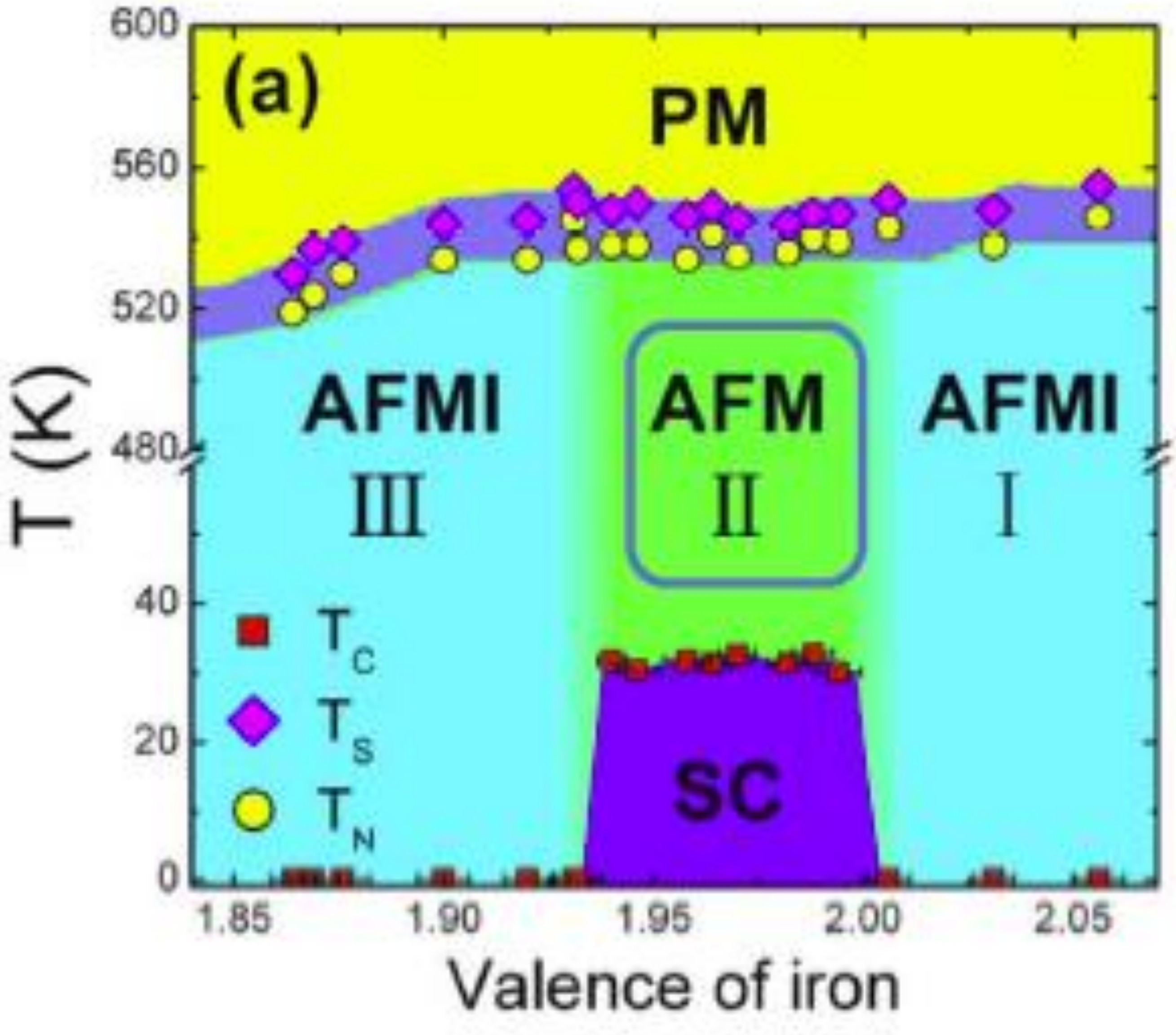

EDCs of $K_xFe_{2-y}Se_2$

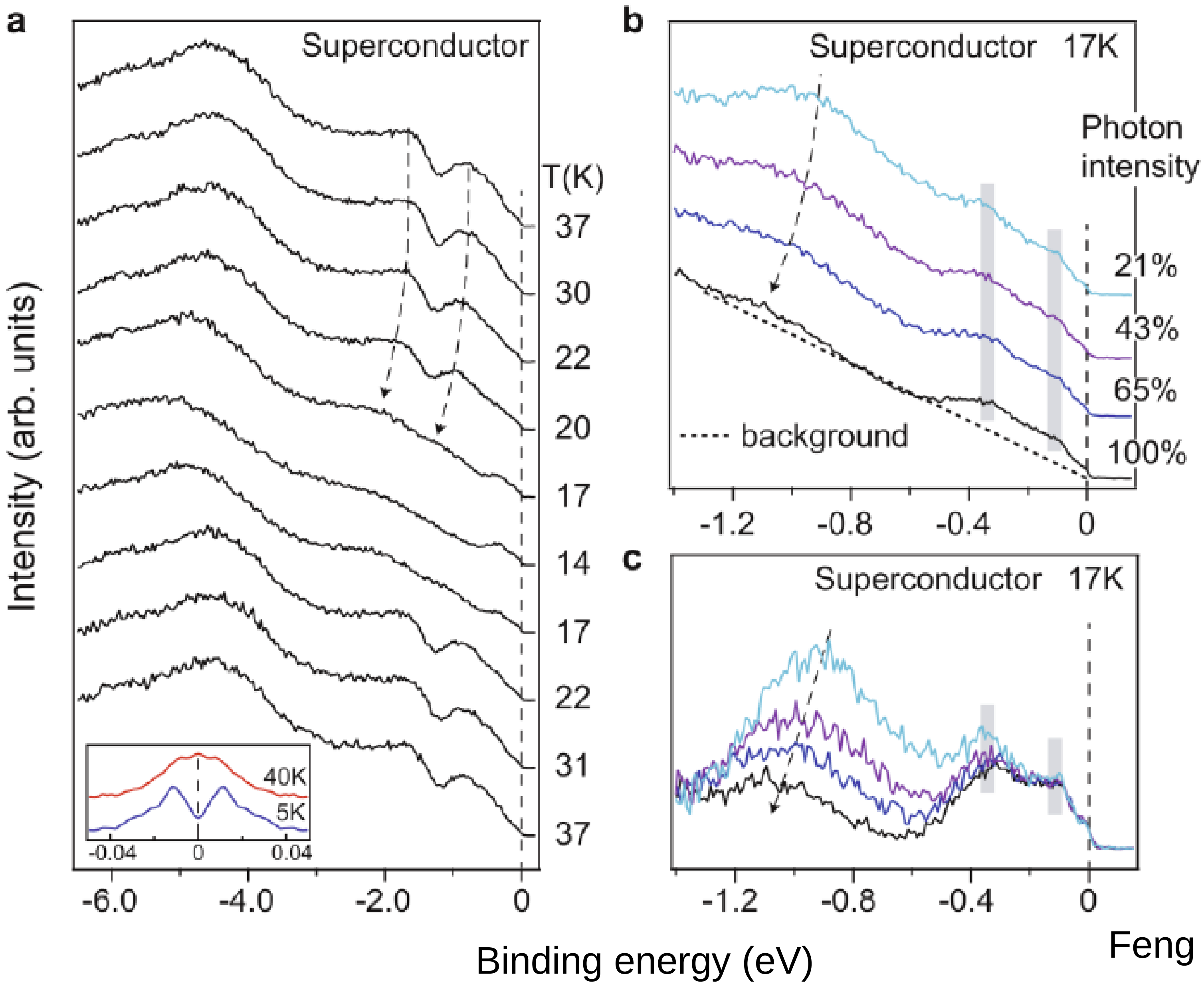

Feng group

EDCs of $K_xFe_{2-y}Se_2$

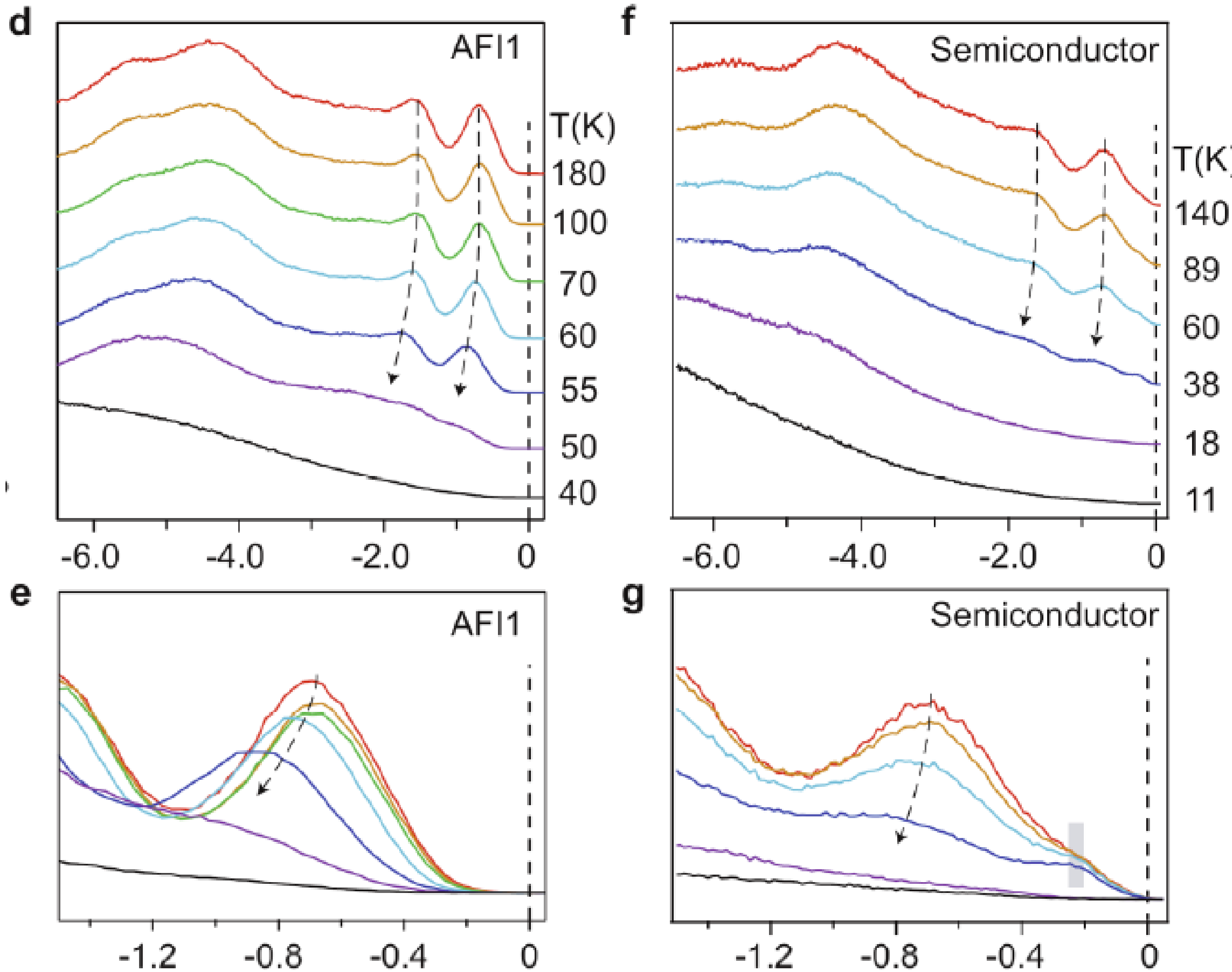

Binding energy (eV)

Feng group

Phase separation in $K_xFe_{2-y}Se_2$

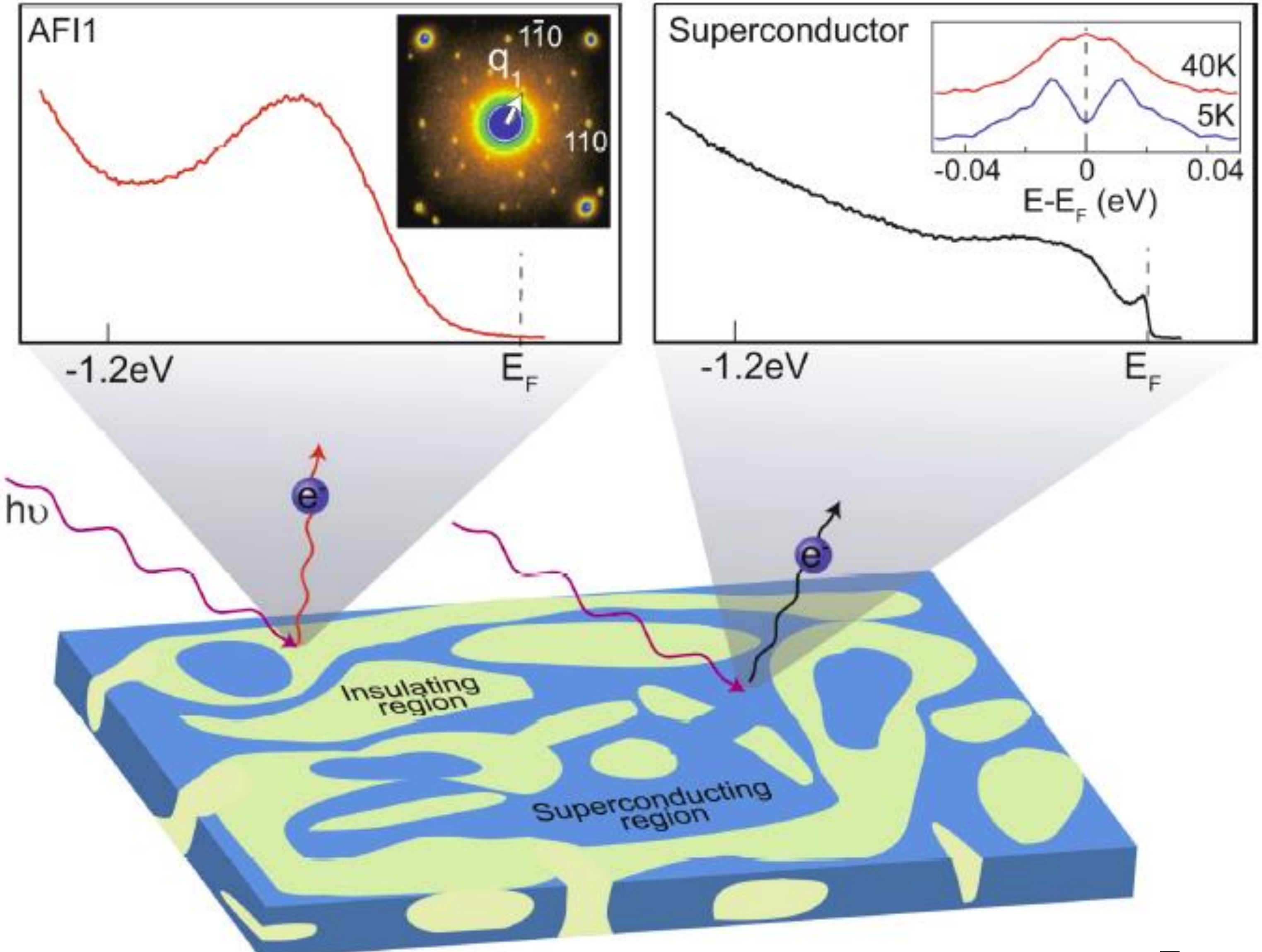

Feng group

Single layer $FeSe/SrTiO_3$

FeSe

Tc~50K

FeAs-122

KFe_2Se_2

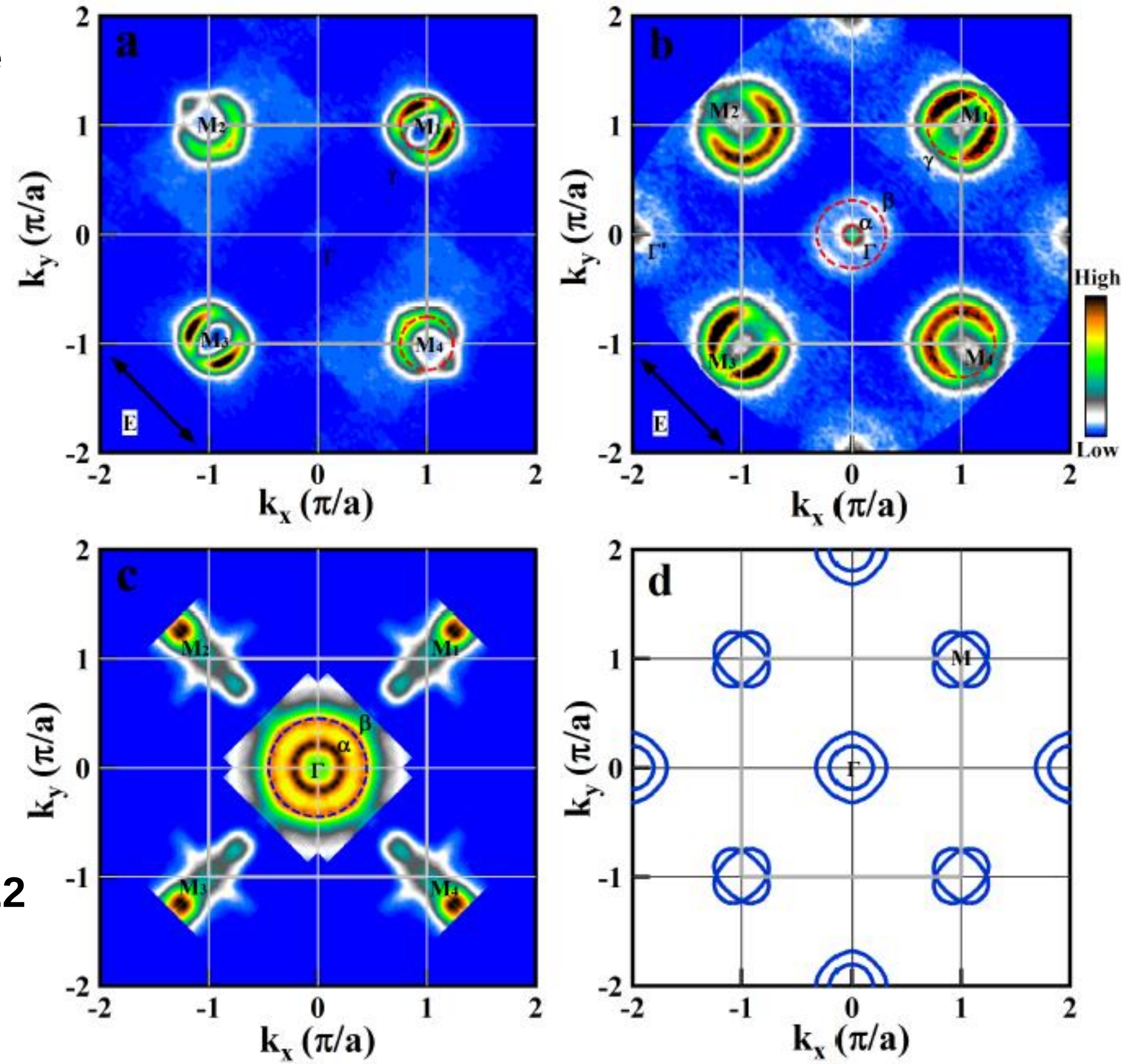

X. J. Zhou Group

Band structure of single-layer FeSe

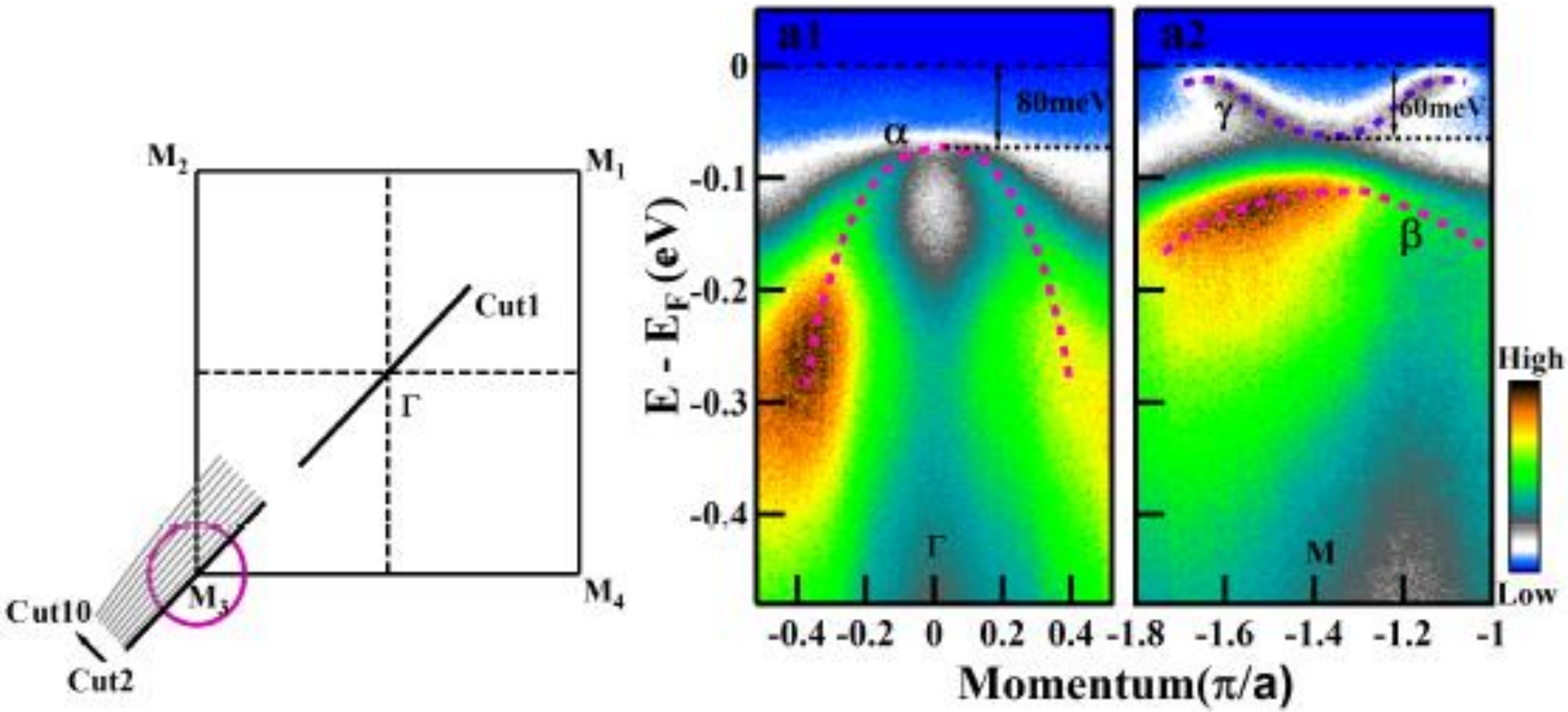

X. J. Zhou Group

Band structure of single-layer FeSe

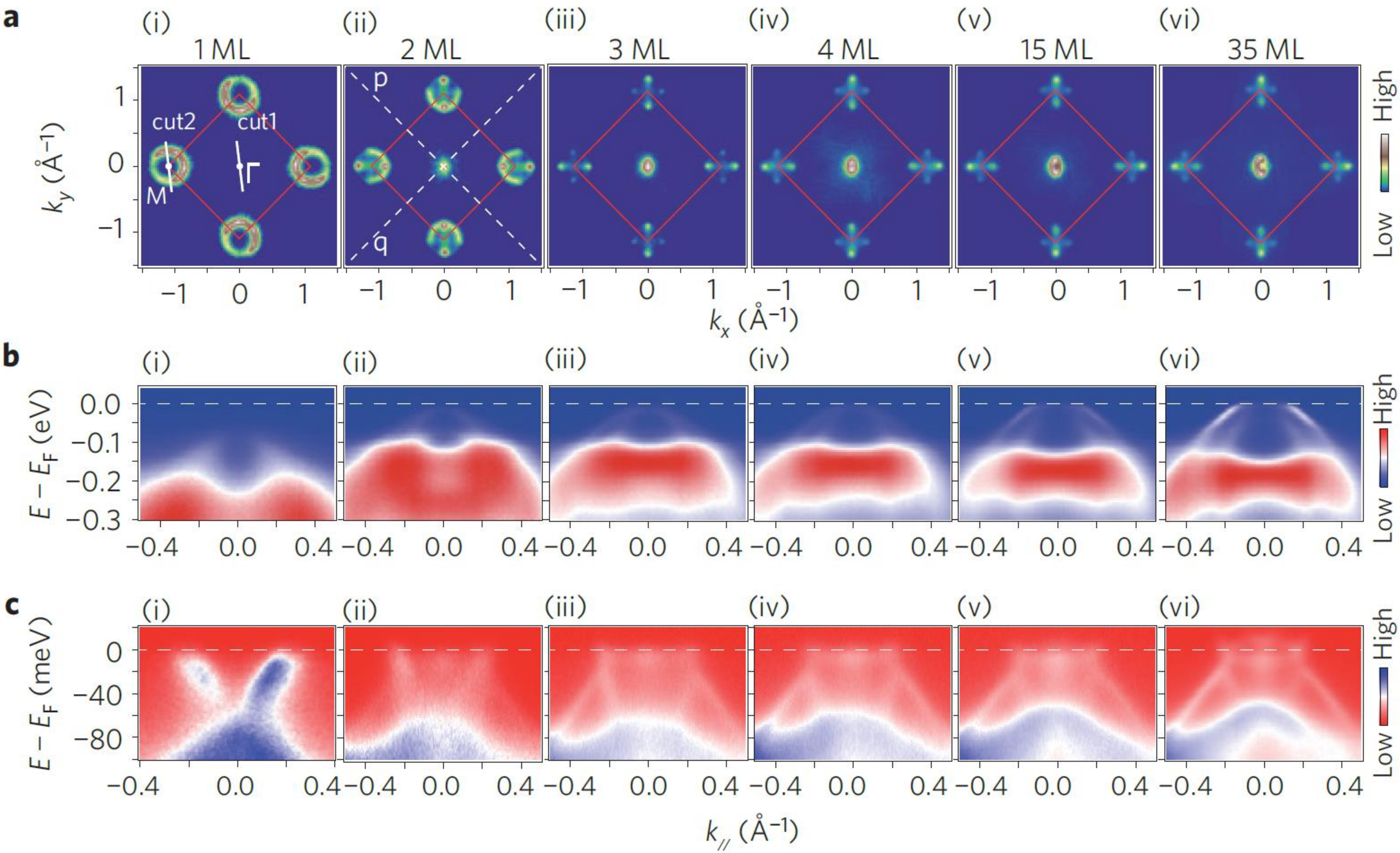

Feng group

Phonons in single-layer FeSe

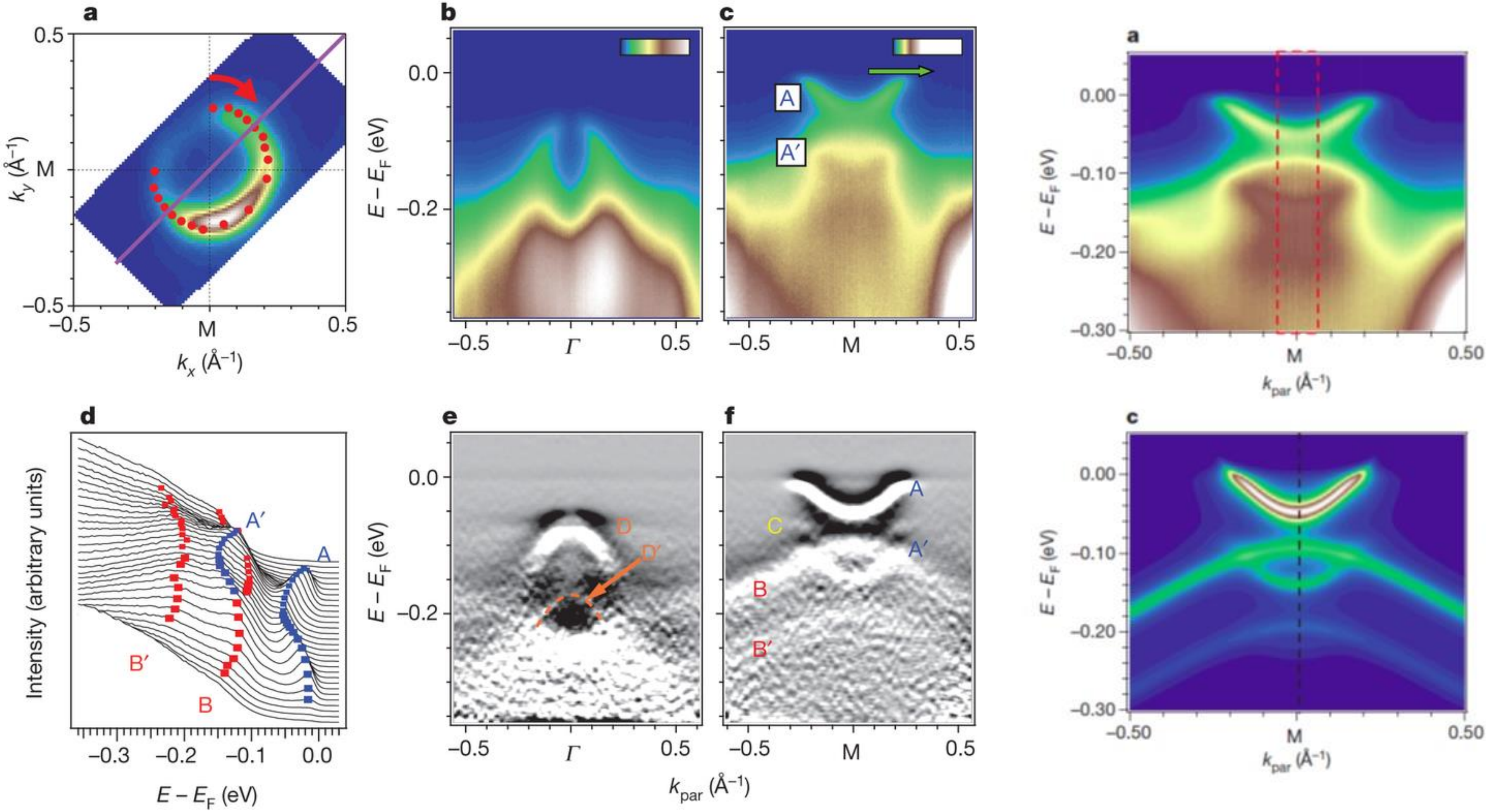

Z. X. Shen group

NaFeAs

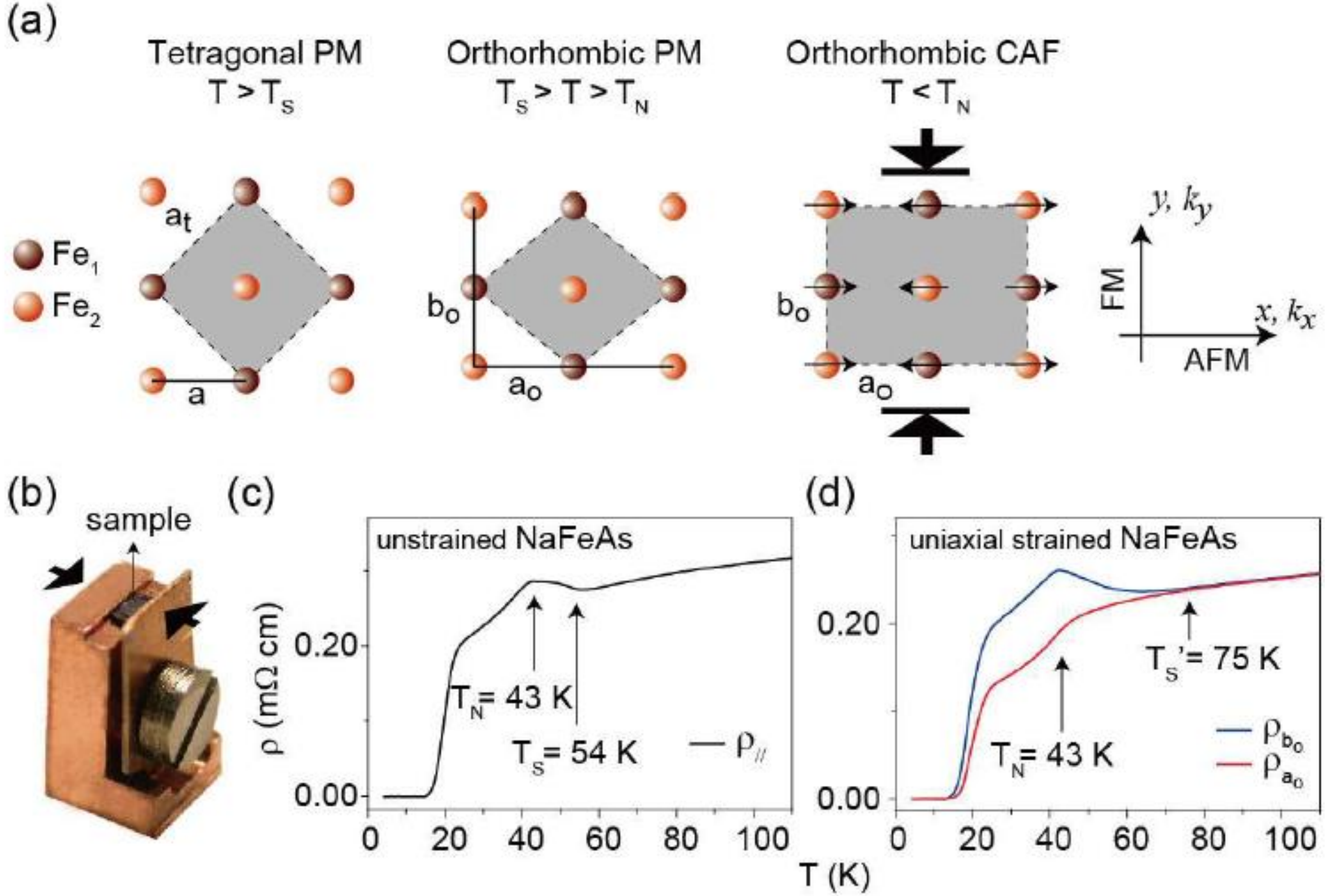

Feng group

Band structure of NaFeAs

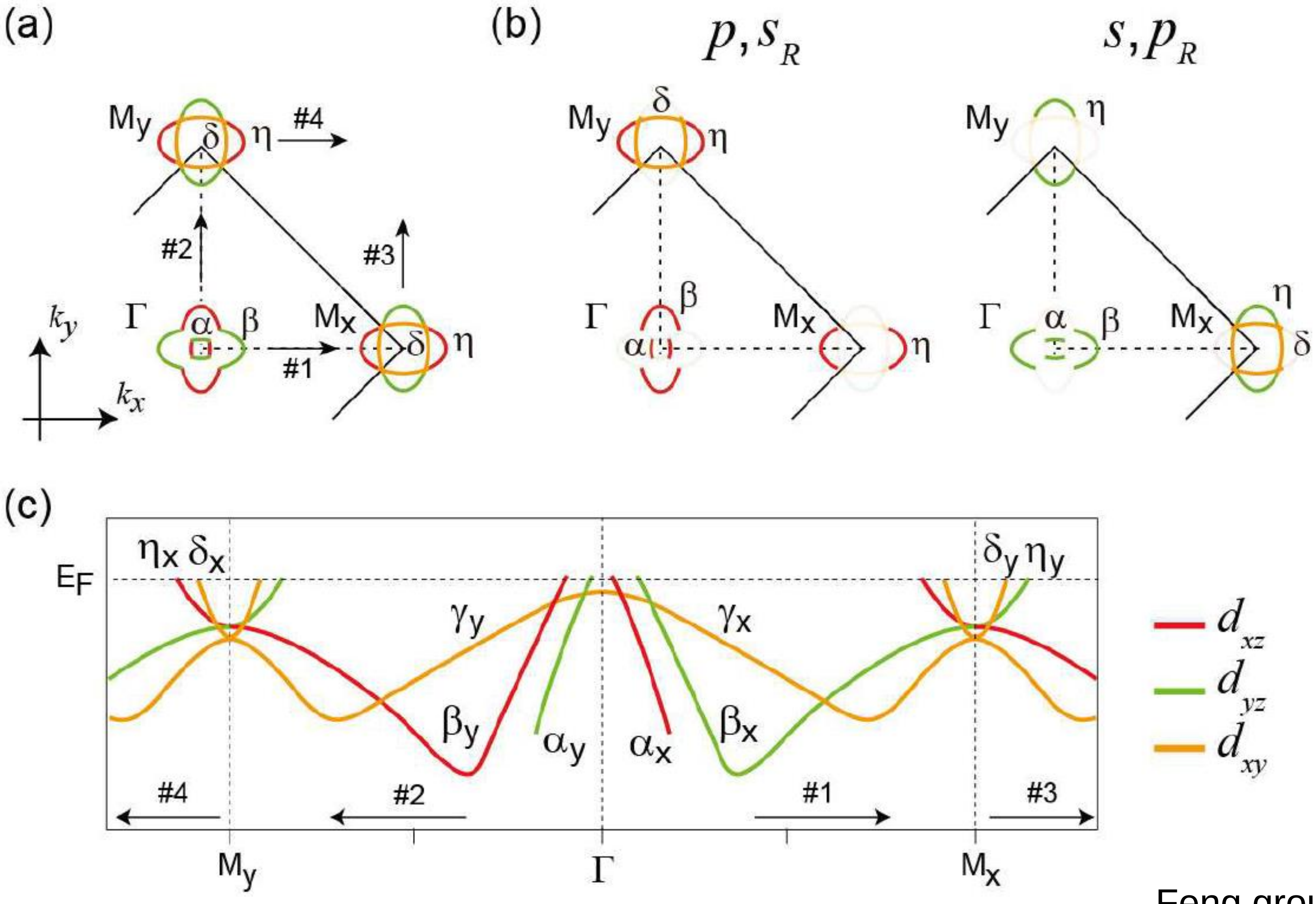

Feng group

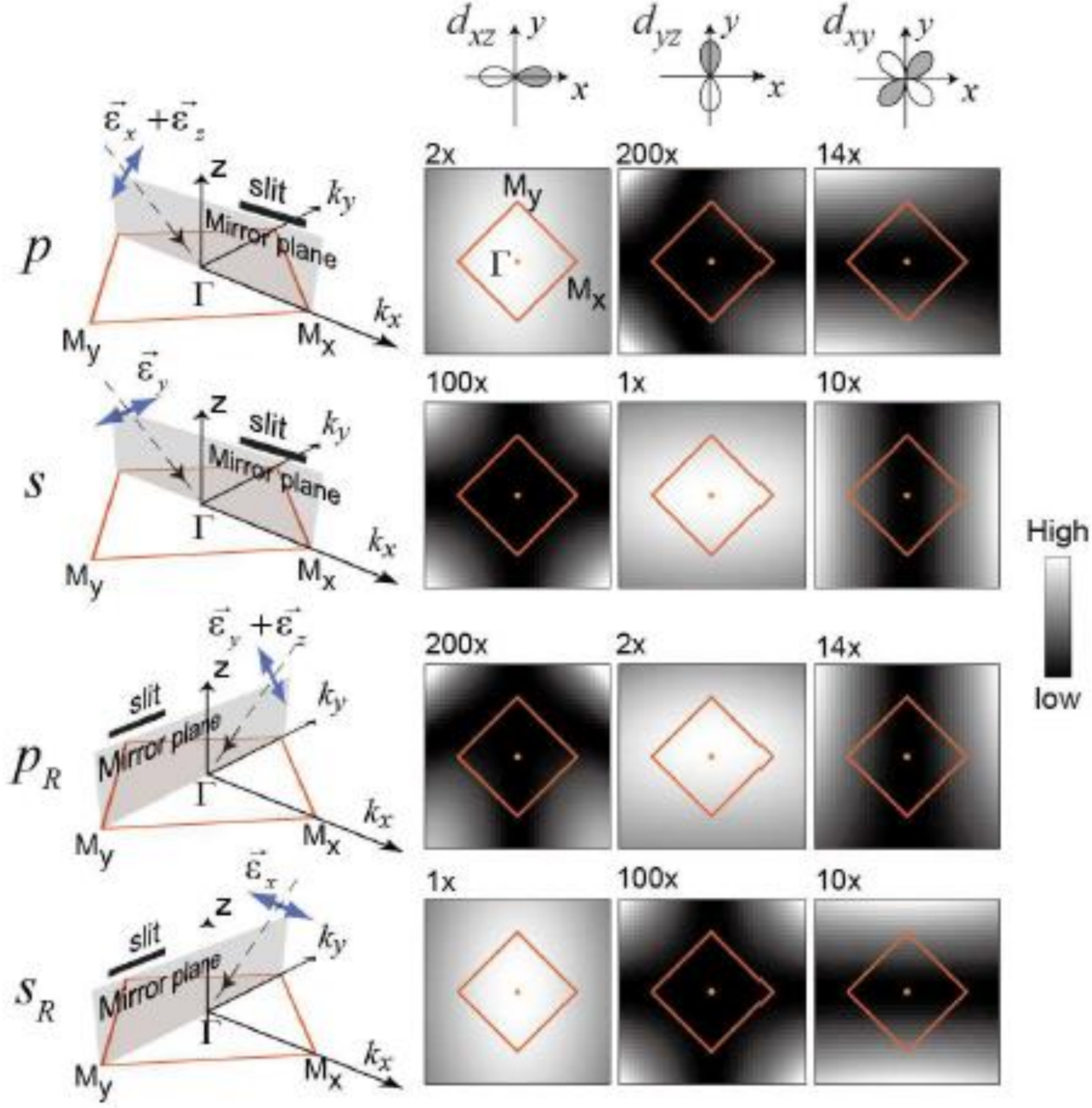

d_{xz}
d_{yz}
d_{xy}
y
x
$\vec{\varepsilon}_x + \vec{\varepsilon}_z$
z
slit
k_y
Mirror plane
k_x
Γ
M_y
M_x
p
s
p_R
s_R
$\vec{\varepsilon}_y$
$\vec{\varepsilon}_y + \vec{\varepsilon}_z$
$\vec{\varepsilon}_x$
2x
200x
14x
100x
1x
10x
High
low

Feng group

$CaFe_2As_2$

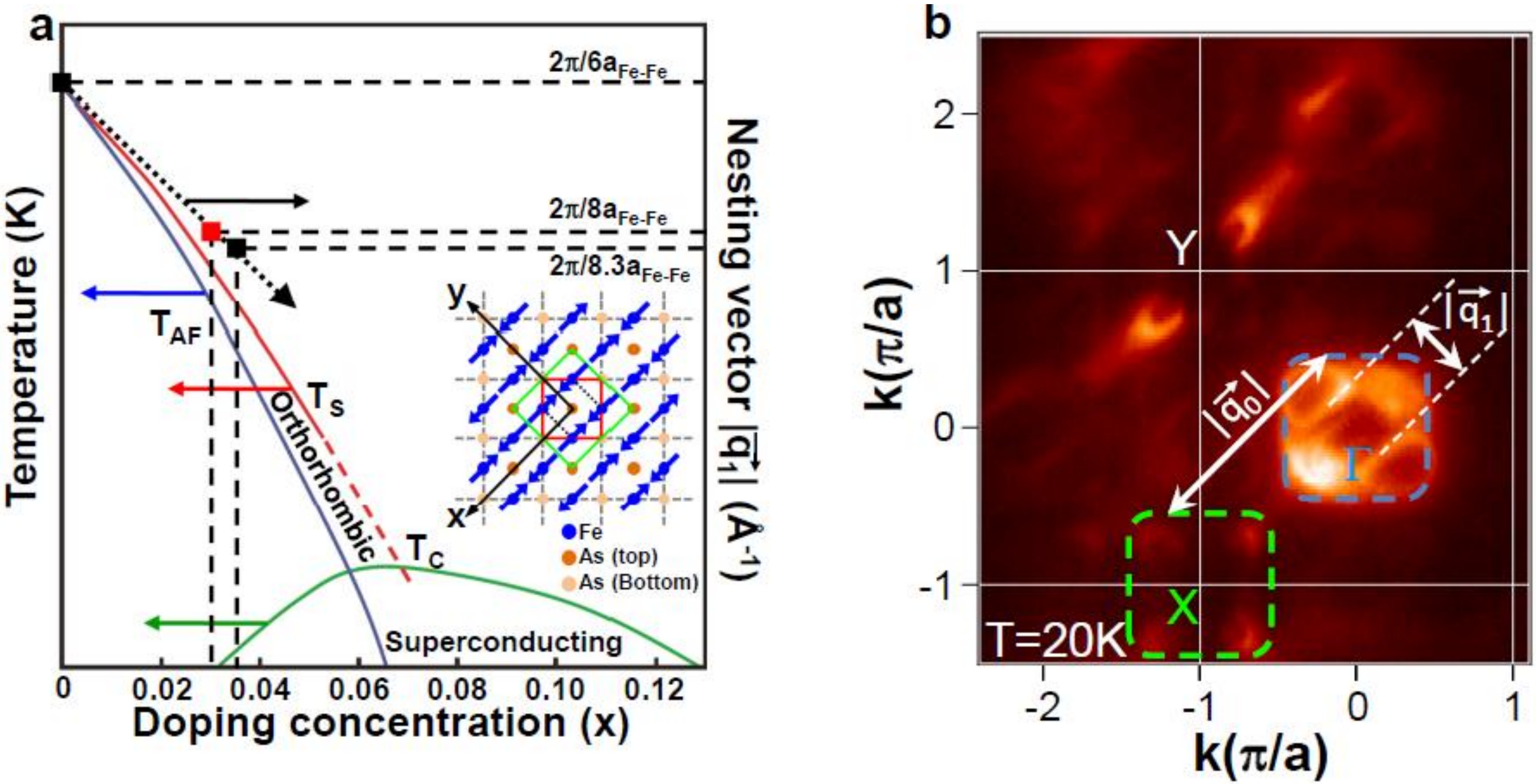
a
$2\pi/6a_{Fe-Fe}$
$2\pi/8a_{Fe-Fe}$
$2\pi/8.3a_{Fe-Fe}$
Temperature (K)
Nesting vector $|\vec{q}_1|$ ($Å^{-1}$)
T_{AF}
T_S
T_C
Orthorhombic
Superconducting
y
x
Fe
As (top)
As (Bottom)
0
0.02
0.04
0.06
0.08
0.10
0.12
Doping concentration (x)
b
Y
Γ
X
$|\vec{q}_0|$
$|\vec{q}_1|$
T=20K
2
1
0
-1
-2
$k(\pi/a)$
$k(\pi/a)$

Fermi surface of $CaFe_2As_2$

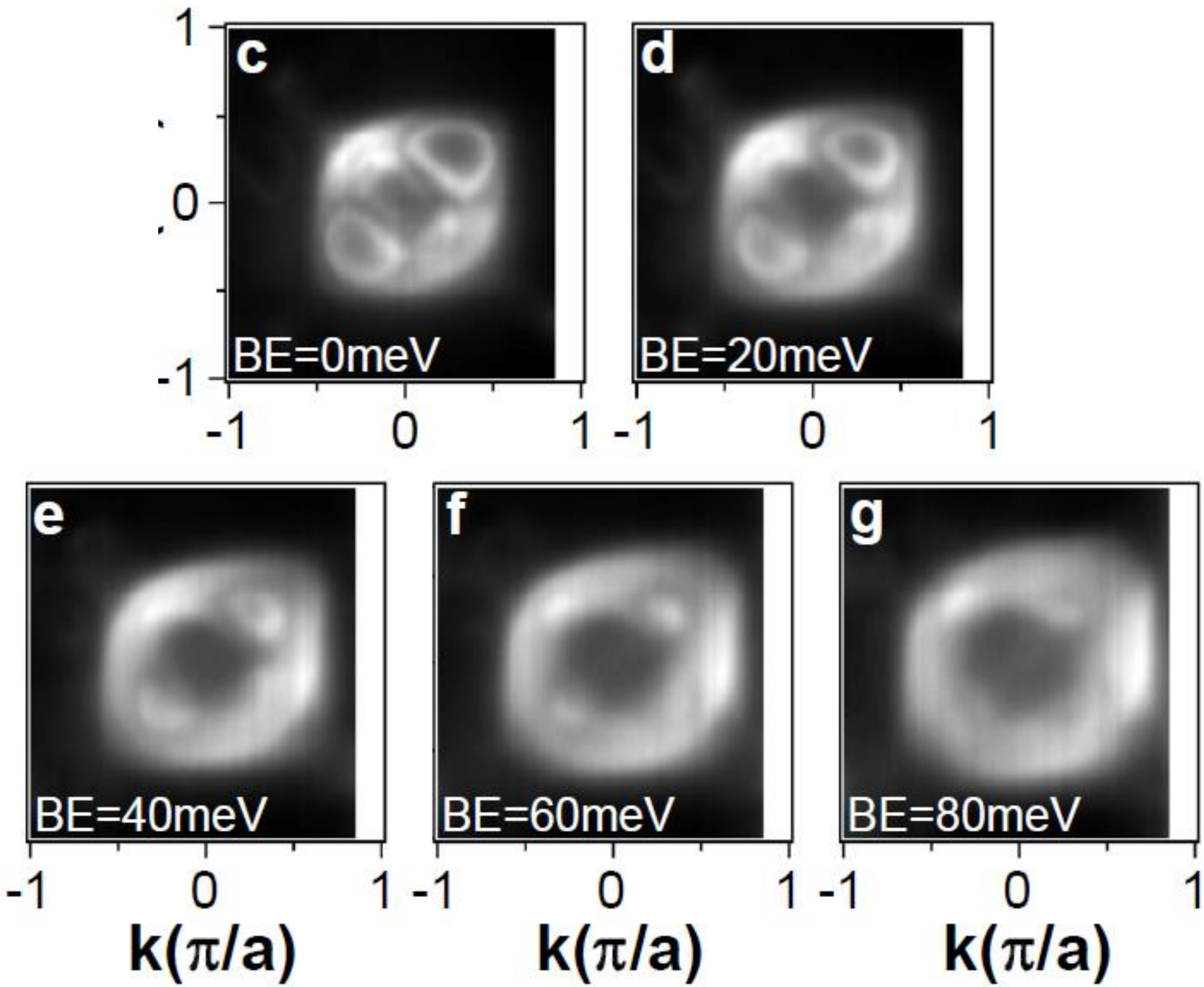

Fermi surface of $CaFe_2As_2$

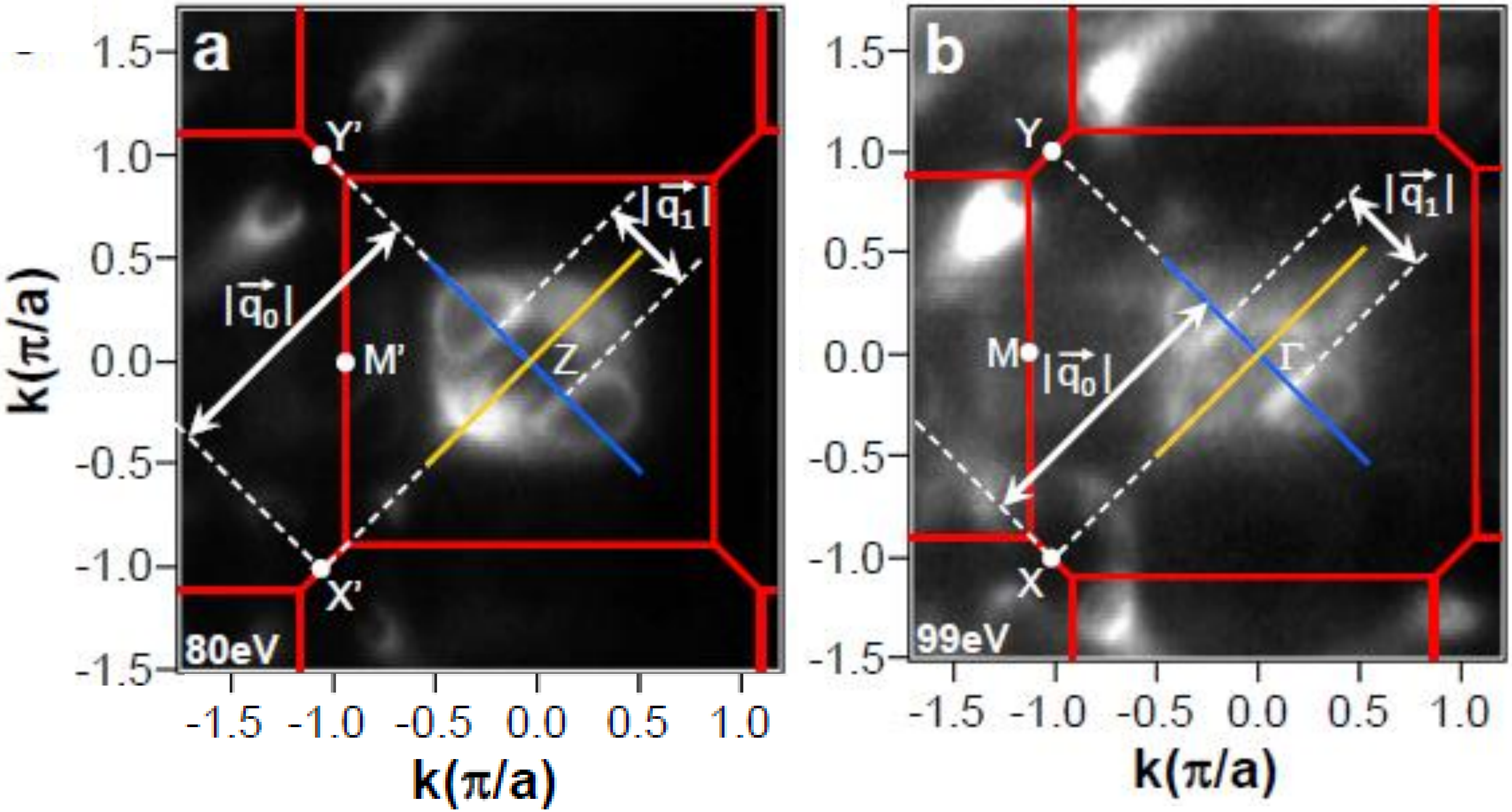

k_z dispersion